NON-CONTACT PLANAR COIL DISPLACEMENT SENSOR

A Project Report

submitted by

VIVEK GANGADHARAN

in partial fulfilment of the requirements
for the award of the degree of

MASTER OF TECHNOLOGY

DEPARTMENT OF ELECTRICAL ENGINEERING
INDIAN INSTITUTE OF TECHNOLOGY MADRAS.

JUNE 2016

THESIS CERTIFICATE

This is to certify that the thesis titled **NON-CONTACT PLANAR COIL DISPLACE-MENT SENSOR**, submitted by **Vivek Gangadharan**, to the Indian Institute of Technology, Madras, for the award of the degree of **Master of Technology**, is a bona fide record of the research work done by him under our supervision. The contents of this thesis, in full or in parts, have not been submitted to any other Institute or University for the award of any degree or diploma.

Dr. Boby George
Research Guide
Associate Professor
Dept. of Electrical Engineering
IIT-Madras, 600 036

Place: Chennai
Date: June 4, 2016

ACKNOWLEDGEMENTS

It gives me great pleasure in expressing my sincere and heartfelt gratitude to my project guide Dr. Boby George for his excellent guidance, motivation and constant support throughout my project. I consider myself extremely fortunate to have had a chance to work under his supervision. It has been a very learning and enjoyable experience to work under him.

Dr. V Jagadeesh Kumar, Head, Measurement and Instrumentation Laboratory, IIT Madras, has been very motivating and supportive. I appreciate Mr. B Umaithanu Pillai, Technical Superintendent, and Mrs. V Rekha, Junior Technical Superintendent, for helping whole-heartedly all the researchers.

My heartfelt appreciation to my lab mates in the Measurement and Instrumentation especially Anish, Srinath, Rohit, Anusha, Aparna, Sandra, Arathi, Shenil ,Anil, Nimal for spending their invaluable time with me, in discussing about the project and answering my queries. Special thanks to Sudhir, Raja, Gashay, Semeer and Ram for your brilliant comments and suggestion.

Words cannot express how grateful I am to my father and mother for all of the sacrifices that you have made on my behalf and the Almighty for uncountable blessings due to which I was able to complete the project on time.

ABSTRACT

KEYWORDS: Inductive Proximity Sensor; Displacement Sensor; Planar Coil; Linearization.

Inspite of large number of displacement sensors available in the market, there are applications that are not met by the existing types of transducers. This lead to development sensors based on new transduction techniques. It has been observed that most of the engineers prefer non-contact, linear, robust, long term reliable and accurate sensors. Considering these factors a novel planar coil position sensor is proposed in this thesis.

The sensor is developed using a planar coil and a target metal (permalloy) having high permeability. When the target metal moves over the coil the magnetic flux density changes and hence the inductance of the coil changes as a sine function of displacement of the metal. The change in inductance causes a proportional change in phase. The phase change recorded and input to the signal conditioning circuit for linearization. To linearize the phase change it is passed through a inverse cosine block. The developed prototype gives a worst-case non-linearity less than 1%.

TABLE OF CONTENTS

LIST OF TABLES

LIST OF FIGURES

ABBREVIATIONS

FEM   Finite Element Method

IPS   Inductive Proximity Sensor

PCB   Printed Circuit Board

PSD   Phase Sensitive Detector

CHAPTER 1

INTRODUCTION

Sensors sense physical or chemical parameter or change in parameter that is of interest in its working environment and then provide an electrical output. Sensors are used in all walks of life and improved the comfort and quality of life. There are enormous number of sensors around us, in our electronic gadgets, vehicles, machines but most of us are not aware of all type of sensors. The advancement in automation elevates the need of different sensors. Engineers continue to use sensors for providing real time information for various measurement and control applications.

There are several kinds of displacement sensors available in the market. These sensors can be classified according to the operating principles such as inductive, capactive, resistive, optical etc. Resistive sensors are the most frequently used displacement sensor. The most common one is potentiometer type. It uses a metallic slider attached to the target whose position or displacement is to be measured and it slides over a highly resistive element. This acts as a potential divider circuit and output is proportional to the slider position. Though the sensor has very simple structure and operation principle,the output deteriorate over period of time due to wear and tear. Capacitive sensor is another important class of sensors that generally contains two plates one is fixed and other is attached to the target which is moving. The change in capacitance produced by the relative change in displacement between the plates produce a change in output. But capacitive sensors cannot be used in harsh environment and is problematic in dusty environment and they are susceptible to humidity change.

Inductive sensor is the most prominent and versatile sensor of all other displacement sensor. It measures the change in inductance caused by the movement of flux concentrating high permeability element. Inductive sensors are non-contact, inherently robust, highly reliable and long lasting. It can be used in harsh and hostile environment. Inductive displacement sensor utilizes high frequency magnetic field which is generated by a high frequency ac signal. As a part of literature survey we came across several methods employed for displacement measurement using inductive transducer. The non-contact

inductive displacement sensor converts linear displacement between the metallic target and sensor head into an electrical analog by observing the change in quality factor with a linearity error of 3% [1]. In another approach to determine the contact force acting on the foot of humanoid robot uses the principle of inductive sensing. The approach has two sets of coils with one fixed coil and one moving coil each. When the moving coil moves over the fixed coil so the inductance changes and the change in inductance can be mapped to displacement [2][3]. The problem with this method is mutual inductance between the coils contribute to the total inductance and concept of partial inductance should be used for the calculation of mutual inductance which is slightly complex [4]. One of the widely used IPS consist of a coil which is wired to a capacitor to get resonance behaviors. The resonance circuit is connected to a oscillatory circuit which provides the feedback necessary for obtaining the feedback condition. The desired information can be extracted from the oscillator signal. Another IPS is developed using eddy current concept[5]. It uses ferromagnetic and paramagnetic targets and coil head arrangement which is connected to the oscillator. Again the oscillator parameters are extracted to get the desired data. There is a modified approach to the above mentioned sensor. It uses a magnet as target material and a specially designed triangular shaped coil. Linearity error is less than 1% [6]. Simulations of inductive displacement sensors by using finite element analysis method(FEM) is useful for extracting parameters to create a compact model of the sensor[7][8].

1.1   Objective

The objective of the project is to develop a non-contact, low cost, miniature size, reliable and accurate inductive displacement sensor. The scheme we proposed is a suitable method to sense displacement or position of the target material. The method does not need rigorous calculations or complex circuitry. Inductive sensor is developed in a PCB this make the sensor planar and easy to mount.

1.2 Organisation of the thesis

Chapter 1 gives an overview of some displacement sensor. The advantages of inductive sensor sensor in harsh and weary environment. A briefing of various existing IPS or displacement sensor and the operating principle is also done.

Chapter 2 describes the design and operating principle of the sensor. It also explains the FEM analysis that we used to fix the final design of the sensor. Chapter 3 describes the measurement setup which include the circuitry and signal conditioning blocks. Chapter 4 details the results we obtained from the prototype developed. Chapter 5 includes conclusions and future scope.

CHAPTER 2

DESIGN AND OPERATING PRINCIPLE OF THE SENSOR
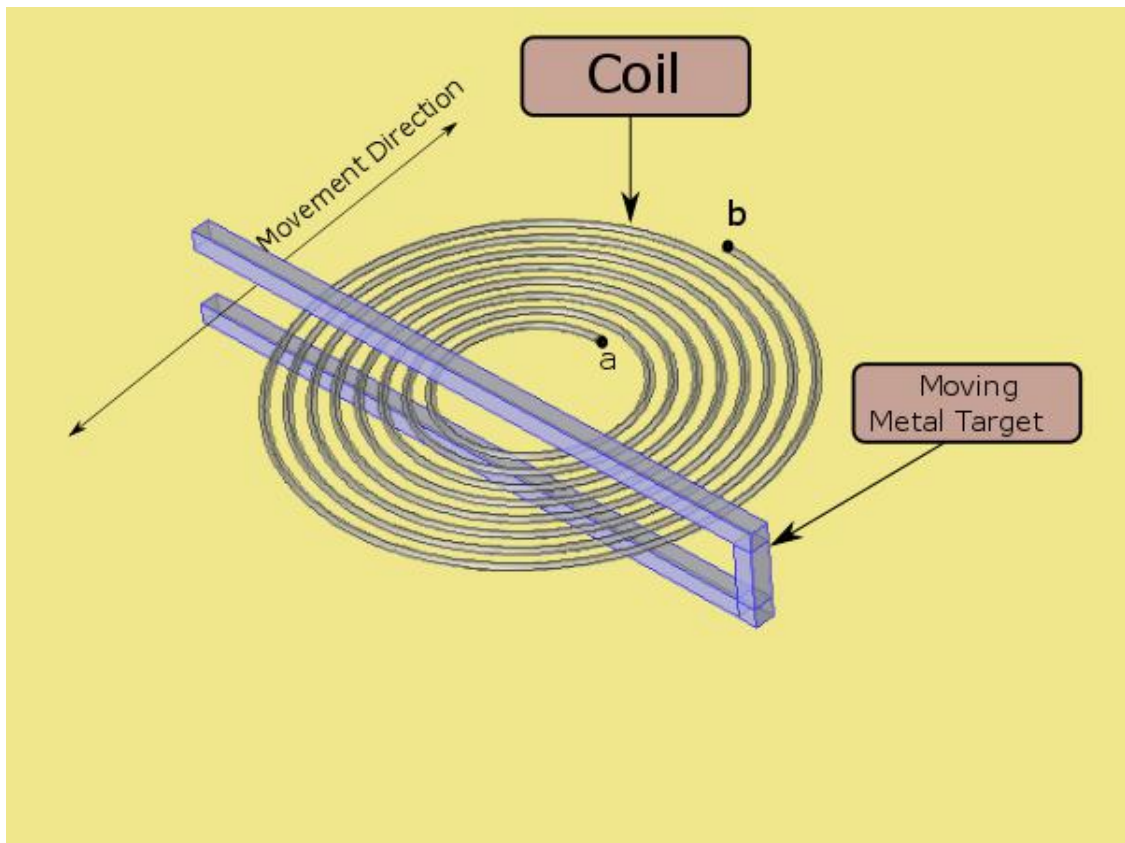
2.1 Sensor Design

Figure 2.1: Proposed Sensor

Fig 2.1 shows the basic design of the sensor. The sensor has a planar coil which is fixed and a U-shaped metallic target of high permeability.The metal moves over the coil. Terminals of the coils are represented as 'a' and 'b'. Undesirable change in inductance due to the vertical movement of the core can be reduce by using U-shaped target.

2.2 Simulation Studies Using Finite Element Modeling

The main components of the sensor is a planar coil fabricated on a PCB and a high permeability metal(permalloy), which is to be placed over the planar coil printed on a PCB. The permalloy metal is moved over the planar coil from one diametric end to the other end. The coil is excited with a suitable ac source. When we move the high permeability target metal over the coil,the permeability changes. The magnetic flux concentrate in vicinity of metal and this causes a rise in magnetic flux density. The change in magnetic flux density changes the inductance. When we move the metal from one coil end to other , the inductance varies as a sinusoidal function of displacement.

The variation of inductance as a sinusoidal function of displacement of the coil is first observed from a simulation done using a FEM analyzing software **COMSOL Multiphysics**. The finite elemental model is shown in the Fig 2.2.

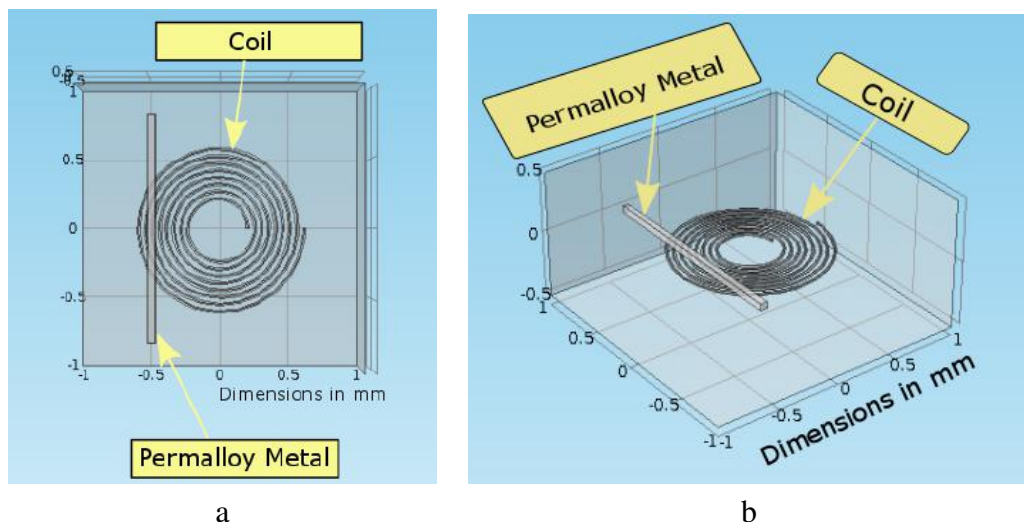a   b

Figure 2.2: a)Top View b)3-D View of Finite Elemental Model

Inductance value is plotted by doing a parametric sweep of position of permalloy metal over the coil. Inductance values obtained at every instant is plotted against the displacement of the metal. Inductance versus displacement plot of the simulation resembled sinusoidal signal pattern. In order to clarify this we did a sine fit using curve fitting tool in **MATLAB** and the curve fit obtained is shown in Fig 2.3.

General model of sine fit is shown below. We can see that R-square value is 0.9988. For exact fit R-square value is 1. The value 0.9988 shows that the fit is very good.
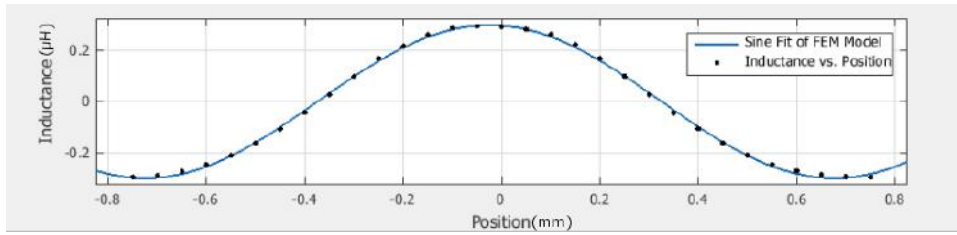
Figure 2.3: Sine Fit of the Finite Element Model using Matlab Curve fit application

General model Sin1:
  f(x) = a1*sin(b1*x+c1)
Coefficients (with 95% confidence bounds):
    a1 =   0.2995 (0.2955, 0.3036)
    b1 =   4.485 (4.446, 4.524)
    c1 =   1.68 (1.666, 1.695)

Goodness of fit:
  SSE: 0.001742
  R-square: 0.9988
  Adjusted R-square: 0.9987
  RMSE: 0.007888

Fig 2.4 shows the concentration of magnetic flux density at different position when the target metal perform a parametric sweep over the coil. It is evident from the figure that the magnetic flux concentrate in the vicinity of the metal. This is the reason for the change in inductance.
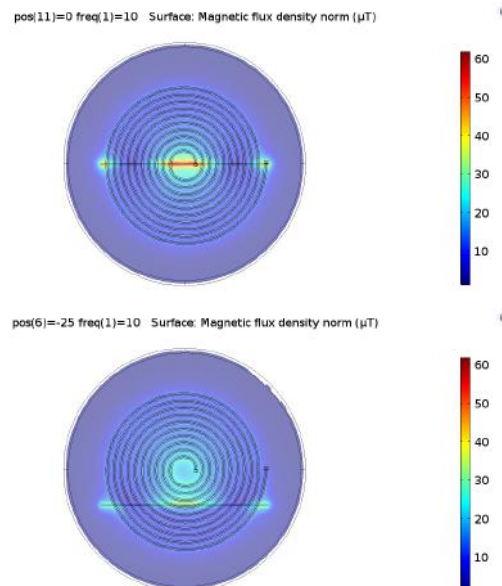

Figure 2.4: Flux density pattern at different locations of target

2.3 Physical Components

2.3.1 Permalloy

Permalloy is a nickel-iron magnetic alloy,with about 80% nickel and 20% iron content. It is notable for it's high magnetic permeability. It has a relative permeability of around 100,000 compared to several thousand for ordinary steel[9]. We are using a U-shaped core made of permalloy as shown in 2.5.
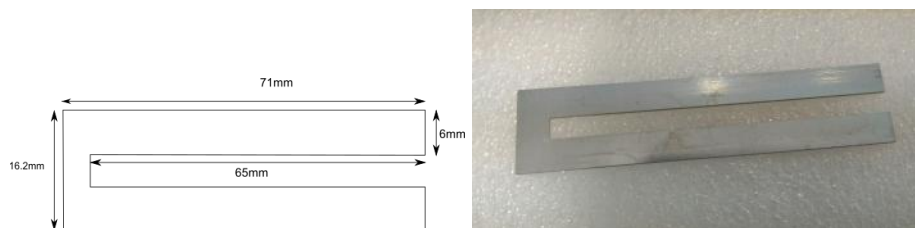

Figure 2.5: U shaped permalloy metal.

2.3.2 Planar coil

Three sets of coils are used in this project. To make the explanation simple let's name the coils as Coil-1,Coil-2 and Coil-3. The coil parameters are specified in the subsequent section. Coils are shown in 2.6.
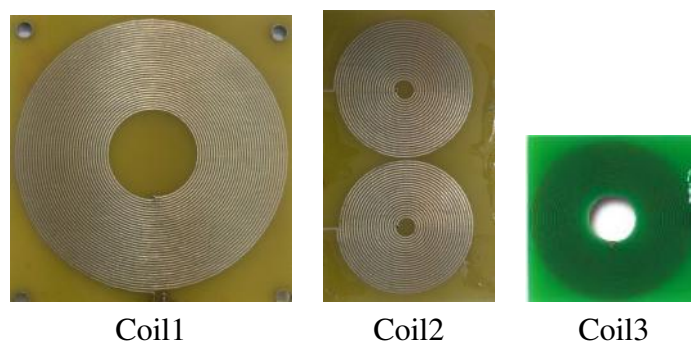

| Coil1 | Coil2 | Coil3 |

Figure 2.6: Planar coils on PCB

2.3.3 Coil Parameter

Coil parameters are given in Table 3.1. Inductance and Resistance are measured using LCR meter at 100kHz.

Parameter	Coil 1	Coil 2	Coil 3
Outer Diameter	$60mm$	$30mm$	$14.5mm$
Inner Diameter	$19mm$	$4mm$	$4mm$
No of Turns	33	21	64
Thickness	$0.3mm$	$0.3mm$	$0.1mm$
Trace width	$0.3mm$	$0.4mm$	$0.1mm$
Inductance	44.645μ	6.5μ	17.5μ
Resistance	12.15Ω	3.780Ω	8.2Ω

Table 2.1: Coil parameter.

Coils printed on PCB are mounted on a stand and permalloy metal is moved over the coil. PCB thickness is 1.6 mm. The clearance between PCB and metal is 0.5 mm. The air gap is very less to reduce the reluctance path. But there will be slight vertical movement of metal due to this air gap which is reduced by placing thin plastic sheet(non conductive) in the air gap.

2.4 Conclusion

Simulation of the sensor was done using FEM software COMSOL Multiphysics. Observed the parameters variation when the metal moves over the planar coil. Variation of inductance of coil was a cosine function of displacement. Curve fitting of the cosine pattern was done using MATLAB curve fitting tool and goodness of fit was found to be good. The coils were fabricated on PCB and target metal was made of a nickel-iron magnetic alloy known as permalloy.

CHAPTER 3

SIGNAL CONDITIONING CIRCUITS AND MEASUREMENT SETUP

We know that one of the prominent parameter of the sensor that varies with the position of target material is the inductance. We can monitor the change in inductance by using a high resolution LCR meter. But from the practical point of view this is not a feasible method since high resolution LCR meter is costly and also the output that we are interested in should a linearly varying signal with displacement of target metal. So we have to use some signal conditioning circuit to get the desired output. Subsequent section discuss about two types of signal conditioning method. First attempt of signal conditioning is by using passive elements alone and in the second method consist of a simple RLC ciruit and LabVIEW VI.

3.1 Method-1

This method was basically analog implementation of trigonometric formula. We are using two identical coils. Both of the coils are placed side by side in a plane but the position of one coil is shifted quarter distance of the coil diameter as shown in the 3.1.

The idea behind shifting the coil is to get inductance of the coils that are 90 degree apart. Lets discuss this idea in detail. The basic idea of this method is to linearize the output proportional to the displacement of target material. Sinusoidal signal with a phase difference of 90 degree is applied to the two coils. That is left coil is supplied with a sine signal and right coil is supplied with cosine signal.

Lets look at the signal conditioning circuit. In the simulation section we have noticed that inductance is varying as a sine function of displacement. So we can represent inductance 'L' as $a*sin(b*x+c)+d$ where x is the variable representing displacement and a,b,c,d are constants. Fig 3.2 represent the signal conditioning circuit of the first method. Inductive sensors L1 and L2 provide feedback path to the opamps. The sources
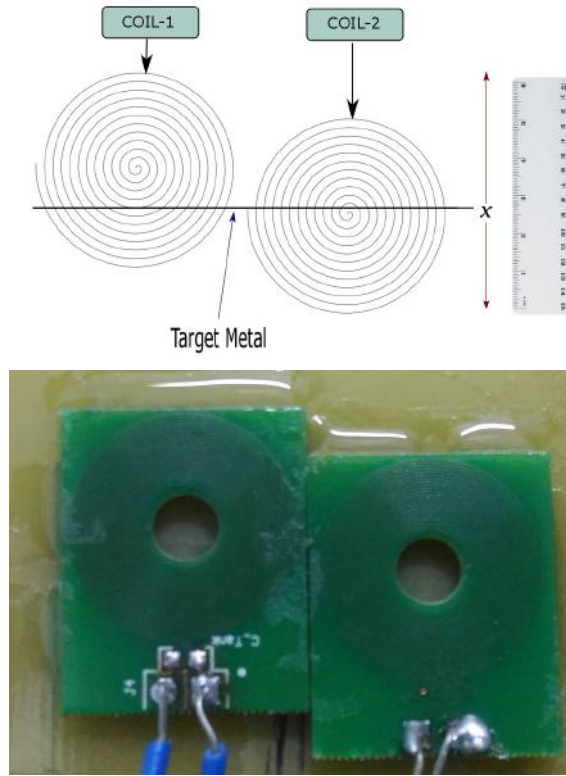
Figure 3.1: Coil placement to get quadrature shifted inductance , x represent the position of target metal

in the second stage of the network and resistors R2 are employed to cancel the offset part in the output equation of the first stage introduced by the offset component 'd' in the inductance equation represented above. Second stage is also used to amplify the output in the first stage. The difference amplifier in the 3rd stage does the subtraction of the signals from the second stage this reduces our trigonometric function and will get the desired format.

$$V_{o1} = -Vm.sin(wt)\frac{jwL1}{Rs} \tag{3.1}$$

$$V_{o3} = Vm.sin(wt)\frac{jwL1}{Rs} - Vm.j.\frac{R3}{R2}.sin(wt) \tag{3.2}$$

$$= Vm.j.sin(wt)\left[\frac{wL1}{Rs} - \frac{R3}{R2}\right] \tag{3.3}$$

$$= Vm.j.sin(wt)\left[\frac{w(a.sin(bx+c)+d)}{Rs} - \frac{R3}{R2}\right] \tag{3.4}$$

$$= Vm.j.sin(wt)\left[\frac{w.a.sin(bx+c)}{Rs} + \frac{w.d}{Rs} - \frac{R3}{R2}\right] \tag{3.5}$$

Inorder to cancel the offset(d) we can select Rs,R2,R3 accordingly.So $Vo3$ is deduced
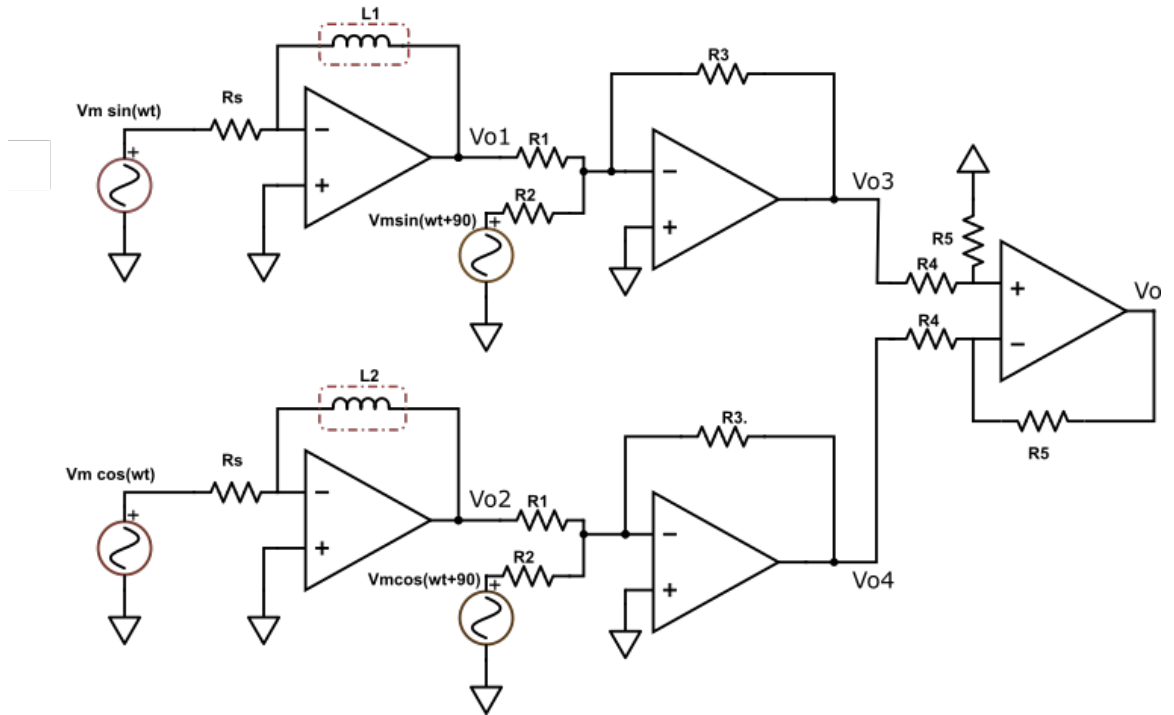
Figure 3.2: Signal Conditioning Circuit

as follows

$$Vo3 \quad = \quad Vm.j.sin(wt) \left[\frac{w.a.sin(bx + c)}{Rs} \right] \tag{3.6}$$

Now Let us consider the other section of the circuit.

$$Vo2 \quad = \quad -Vm.cos(wt) \frac{jwL2}{Rs} \tag{3.7}$$

$$Vo4 \quad = \quad Vm.cos(wt) \frac{jwL2}{Rs} - Vm.j.\frac{R3}{R2}.cos(wt) \tag{3.8}$$

$$= \quad Vm.j.cos(wt) \left[\frac{wL2}{Rs} - \frac{R3}{R2} \right] \tag{3.9}$$

$$= \quad Vm.j.cos(wt) \left[\frac{w(a.cos(bx + c) + d}{Rs} - \frac{R3}{R2} \right] \tag{3.10}$$

$$= \quad Vm.j.cos(wt) \left[\frac{w.a.cos(bx + c)}{Rs} + \frac{w.d}{Rs} - \frac{R3}{R2} \right] \tag{3.11}$$

Similarly $Vo4$ can be deduced as

$$Vo4 = Vm.j.cos(wt) \left[\frac{w.a.cos(bx + c)}{Rs} \right] \tag{3.12}$$

11

Now consider the output of the difference amplifier

$$Vo = Vo3 - Vo4 \tag{3.13}$$

$$= Vm.cos(wt)\left[\frac{w.a.sin(bx+c)}{Rs}\right] + Vm.sin(wt)\left[\frac{w.a.cos(bx+c)}{Rs}\right] \tag{3.14}$$

$$= \frac{Vm.w.a}{Rs}[cos(wt).sin(bx+c) + sin(wt).cos(bx+c)] \tag{3.15}$$

$$= \frac{Vm.w.a}{Rs}[sin(wt+bx+c)] \tag{3.16}$$

Lets replace bx+c by ϕ.So (2.16) will become
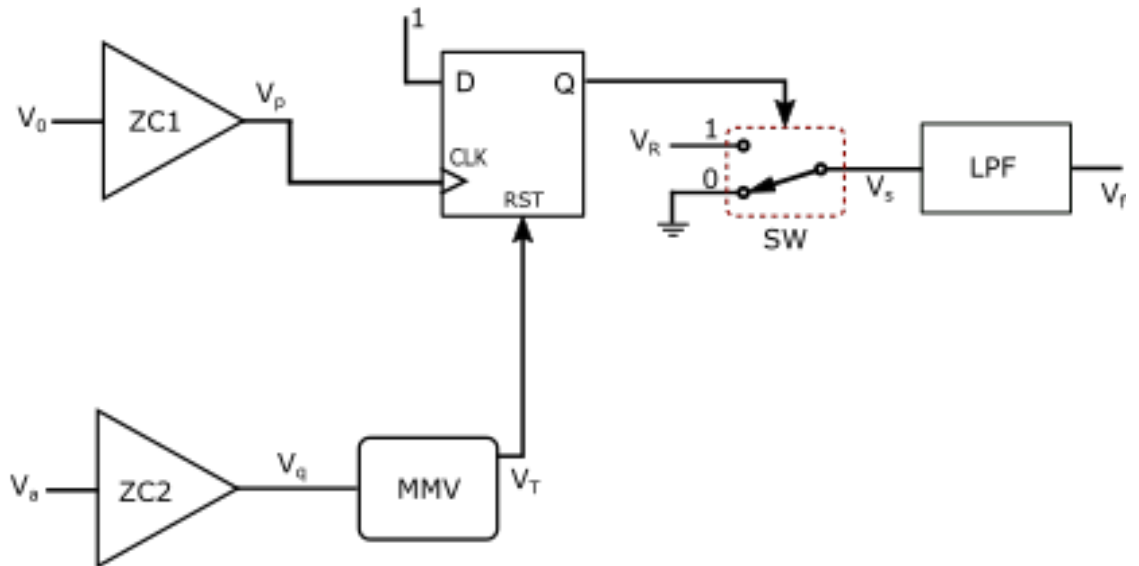
$$Vo = \frac{V_m.w.a}{Rs}[sin(wt+\phi)] \tag{3.17}$$

Figure 3.3: Phase detector

From (3.17) we can observe that to get an output proportional to displacement we require a phase detector to extract ϕ. Fig 3.3 shows a phase detector that gives a voltage proportional to ϕ. Input of the first zero crossing detector(ZC_1)is the output from the passive network which is represented as V_0 and input to second zero crossing(ZC_2) detector is a reference sinusoidal signal $V_a = V_A sin(\omega t)$. Output of ZC_2 is given to the input of Mono stable multivibrator(MMV). Rising edge triggered MMV produce a pulse of small duration and is drawn by the reset terminal of the D-latch. Whereas output of ZC_1 is supplied to the clock terminal of the D latch. The input of D-latch is always 1 so it is bypassed to the output whenever clock is high. D-latch output(Q)controls

the SPDT switch(SW). If Q is 1 SW selects voltage V_R and if Q is 0 it selects ground voltage. Final block in the circuit is a low pass filter(LPF) which takes average of the pulse signal from SW.
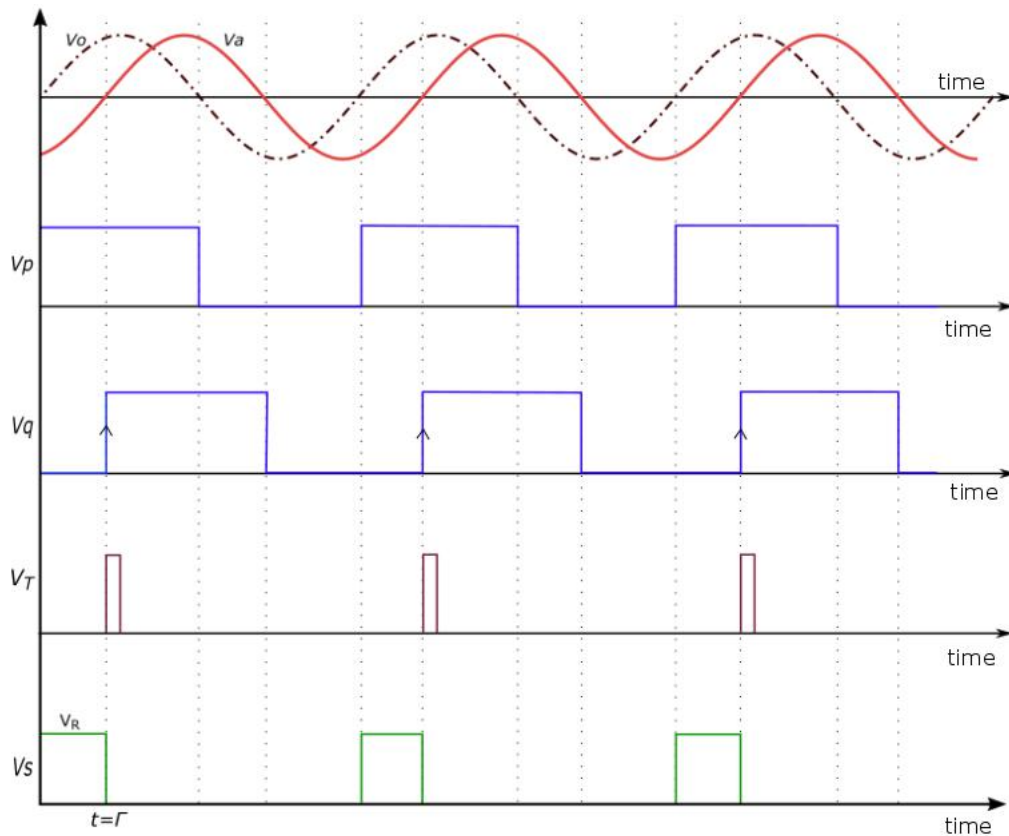

Figure 3.4: Wave forms at quiescent points of the phase detector

In Fig.3.4 V_o represent the output from the passive circuit that we have seen above and V_a represent the reference voltage which is also a sinusoidal signal with phase zero. V_p which is the output of the zero crossing detector(ZC1) is connected to the clock of D latch whose input is wired to logic high. So whenever clock(V_p) is high Q gets D value. The output of the latch acts as a control signal to the SPDT switch SW. As long as V_p is high switch selects terminal one so low pass filter(LPF) gets a reference DC voltage(V_R) as input. On the other hand the ouptut of zero crossing detector ZC2 triggers the positive edge triggered Mono Stable Multivibrator(MMV). The narrow pulse produced by MMV reset the D latch. The switch toggle and selects the ground signal and fed it to the LPF input. This process continues,thus providing a pulse train $\Gamma = (\frac{T}{360})\phi$ if ϕ is expressed in degree(or $\Gamma_\phi = (\frac{T}{2\pi})\phi$ if ϕ is in radian) as input to the LPF. The output V_f of the LPF will be the average value of its input pulse

train and can be derived as

$$V_f \;=\; \frac{1}{T}\left[\int_0^{\Gamma} V_R\,dt + \int_{\tau}^{T} 0\,dt\right] = V_R.\left[\frac{\Gamma}{T}\right] \tag{3.18}$$

Substituting the value of Γ in (2.19), results in

$$V_f \;=\; V_R\left[\frac{\Gamma}{T}\right] \tag{3.19}$$

$$V_f \;=\; \frac{V_R}{360}\phi \tag{3.20}$$

Substituting value of ϕ in (2.20),

$$V_f \;=\; \frac{V_R}{360}(bx + c) = K_T.x \tag{3.21}$$

If ϕ is expressed in radians, then $V_f = \frac{V_R}{2\pi}(bx + c)$. As can be seen from (2.21) the final output V_f of the signal conditioning circuit ,and hence the output of the sensor varies linearly with displacement. That is,when x=0,$V_f = \frac{V_R}{2\pi}c$ and as displacement(x) increases V_f increases linearly since V_R,2π,b and c are constants[10].

But in this method we missed to consider the coil resistance(R_m). Let's rewrite the equations by considering this also.

$$Vo1 \;=\; -Vmsin(\omega t)\left(\frac{j\omega L1 + Rm}{Rs}\right) \tag{3.22}$$

$$=\; -Vmsin(\omega t)\left(\frac{Rm}{Rs} + \frac{j\omega L1}{Rs}\right) \tag{3.23}$$

$$Vo3 \;=\; \frac{Rm + j\omega L1}{Rs}.\frac{R3}{R1}.Vmsin(\omega t) - Vmcos(\omega t).\frac{R3}{R2} \tag{3.24}$$

$$=\; \frac{Rm.R3}{Rs.R1}Vmsin(\omega t) + Vmcos(\omega t)R3\left[\frac{\omega.L1}{Rs.R1} - \frac{1}{R2}\right] \tag{3.25}$$

similarly we will obtain expression for Vo2 and Vo4

$$Vo2 \;=\; -\left(\frac{Rm + j\omega L2}{Rs}\right)Vmcos(\omega t) \tag{3.26}$$

$$Vo4 \;=\; \frac{R3.Rm}{R1.Rs}Vmcos(\omega t) - R3.Vmsin(\omega t)\left[\frac{\omega L2}{R1.Rs} - \frac{1}{R2}\right] \tag{3.27}$$

Before going to the third stage which is the difference amplifier we have to verify the results. If we check (3.25) using PSD method such that the reference signal is

14

$Vmsin(\omega t)$ then the output cosine component should be constant if we assume Rm is not changing and the sine component should change since inductance is changing. But while examining the result it was observed that cosine component is changing. So our assumption that Rm will remain constant through out was wrong similar observation was obtained for $Vo4$ too.

The problem with this method is while considering the resistance of the sensor the equation become too complex and also the resistance(Rm) also varies like inductance as we slide the metal over the coil. Also the quadrature placement of the coil to obtain 90 degree phase shifted inductance between the two coils was also not easy. This made us to think about another circuit which is less complex and this leads to the second method which is explained in the next section.

3.2   Method-2

We know it is difficult to measure the change in inductance directly. So we are using a series RLC circuit and output is drawn across resistor. Let's refresh the basics of RLC network. Fig3.5 shows the RLC network that we are using.
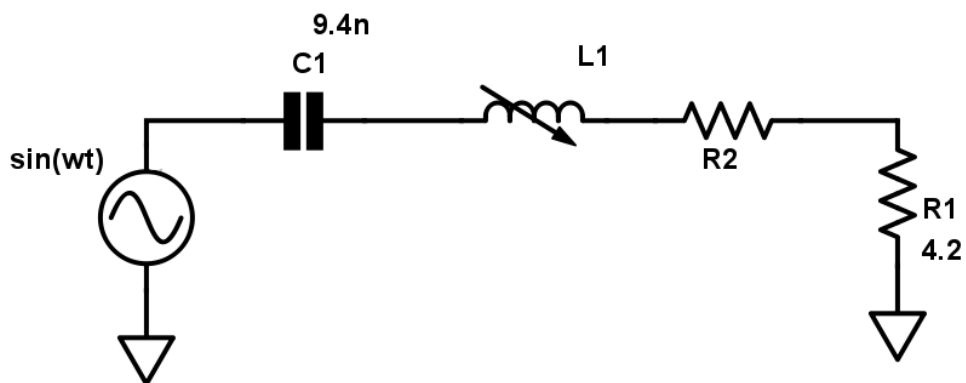

Figure 3.5: Series RLC

Let V_S be the source voltage,V_R,V_C,V_L be the voltage across the resistor,capacitor and inductor respectively. R_2 represent the resistance of the coil and R_1 represent output

resistance.

$$V_S \quad = \quad V_R + V_L + V_C \tag{3.28}$$

$$V_S \quad = \quad IZ_R + IZ_L + IZ_C \tag{3.29}$$

$$= \quad IR + I.jX_L + I. - jX_C \tag{3.30}$$

$$= \quad I(R + j(X_L - X_C))Z = \frac{V_S}{I} = R + j(X_L - X_C) \tag{3.31}$$

$$\tag{3.32}$$

Magnitude and phase of (2.26) can be represented as

$$|V| \quad = \quad \sqrt{V_R^2 + (V_L^2 - V_C^2)} \tag{3.33}$$

$$\theta \quad = \quad tan^{-1}\frac{X_L - X_C}{R} \tag{3.34}$$

Fig 3.6 shows the coil and metal arrangement. Inductance varies as a cosine function of displacement. When the metal is not above the coil but in the vicinity of coil the inductance will take a nominal value. When we move the metal the inductance increases and will attain the maximum inductance value when the metal is exactly above the center of the coil. If we move the metal again then inductance will reduce and it takes the nominal value when the metal reaches the coil edge. So it is evident that the nominal value is the minimum value of inductance while considering the range of displacement as the diameter of the coil.

Basic idea of this method is to fix resonance at a position which is the quarter of the coil diameter that is if L is the diamter we have to choose L/4. To get the resonance frequency at this particular position a bode analyzer is utilized. Input voltage and output voltage(voltage across resistor R1). Now fed the RLC circuit with this resonant frequency. Now let's recall some of the property of resonance. At resonance the applied voltage and the resultant current are in phase. The total impedance of the circuit is pure resistive

$$Z \quad = \quad R + j(0) \tag{3.35}$$
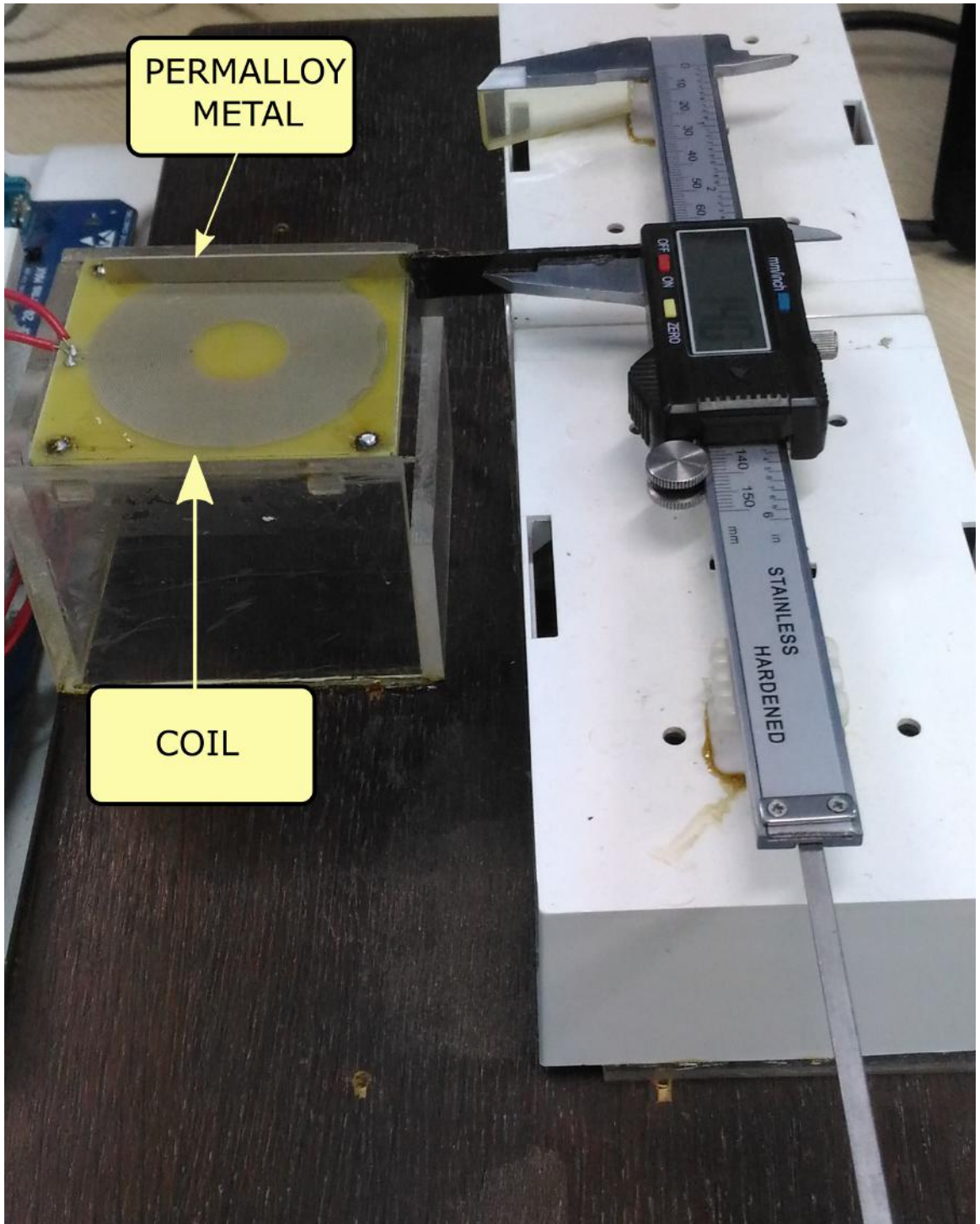
$$Z \quad = \quad R + j(X_L - X_C) \tag{3.36}$$

Figure 3.6: Prototype and Experimental Setup

Combining (2.29) and (2.30)

$$X_L - X_C = 0 \tag{3.37}$$

$$w.L = \frac{1}{w.C} \tag{3.38}$$

$$w^2 = \frac{1}{L.C} \tag{3.39}$$

From (2.28) At resonance,phase(θ) is 0. When we move the coil from one outer edge to center the inductance of the coil increases. So it satisfies the following equations.

$$Z = R + j(X_L - X_C) = |Z| < \theta \tag{3.40}$$

$$I = \left|\frac{V}{Z}\right| < -\theta \tag{3.41}$$

The equation says that if we move the metal from outer edge to center then the phase will change from positive values to negative values. We will get highest positive phase at the edge and negative phase at center of the coil. From center to other edge the change in phase follows the same trend.

3.2.1 Component Selection

The nominal inductance value of the coils is in the range of micro Henry. The sensitivity of the sensor depends on the frequency of input signal and Resistance in the circuit. Let's verify it using equations given below.

$$\theta = tan^{-1}\frac{X_L - X_C}{R} \tag{3.42}$$

$$= tan^{-1}\frac{wL - \frac{1}{wC}}{R} \tag{3.43}$$

$$= tan^{-1}\frac{w^2LC - 1}{wRC} \tag{3.44}$$

Also,as better the Q-factor better is the sensitivity of the sensor. $Q = X_L/R = wL/R = Resonant Frequency/BandWidth$. From the sets of equation we can claim that the two parameters that effect sensitivity is Frequency and Resistance. Considering the above fact we should select a high resonant frequency. So capacitance value should be less but there are constrains. Frequency of input signal is limited by the sampling rate. We should select a capacitor value taking these factors into account.

Now the second factor is resistance across which the output is taken should be very low. The change in sensitivity can observed from 3.7. But as we keep on reducing the output resistance the loading effect will increase. Considering all these factors we have selected capacitor of 9.4nF and resistance of 10Ω.

Let's observe 3.8 which represent the resonant frequency of coil from the bode plot obtained using the bode analyzer.
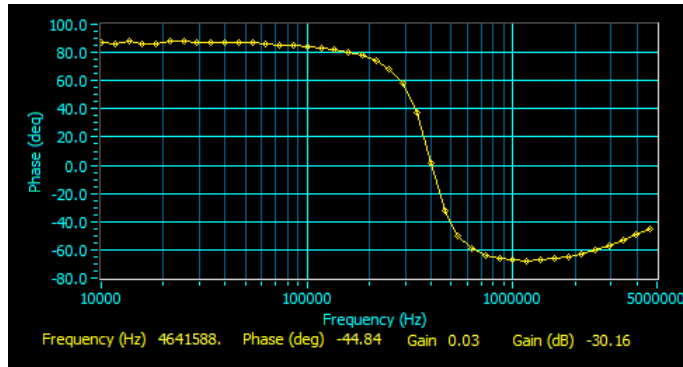
(a)
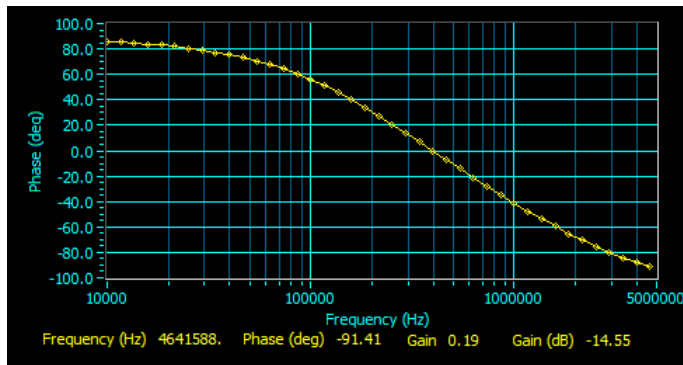
(b)

Figure 3.7: Sensitivity of sensor a)When resistance is 10Ω b)When resistance is 100Ω
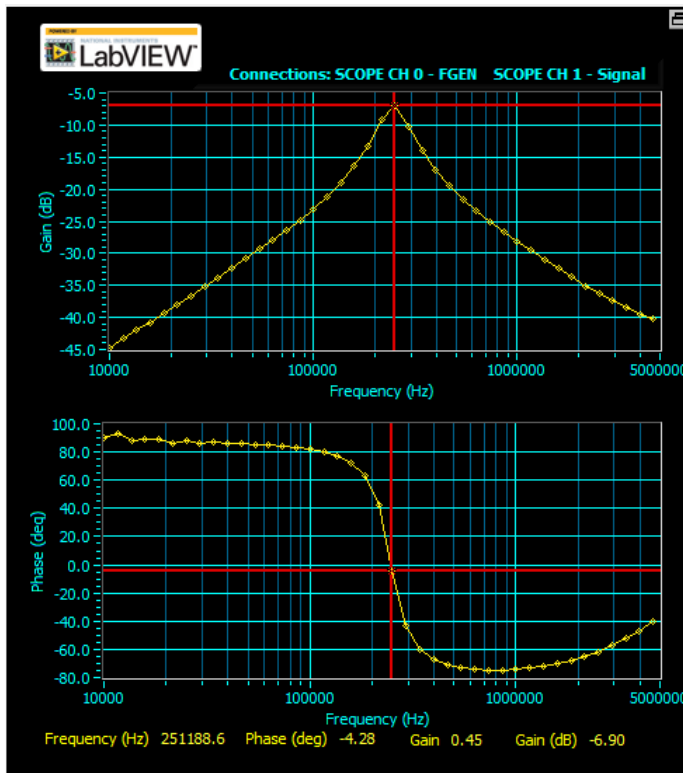

Figure 3.8: Bode plots of coil obtained using bode analyzer

3.2.2 Signal Conditioning

Previous section explained how to select the components. Now let us examine the signal conditioning we used in the project. We know that high precision LCR meter is needed to measure the change in inductance of the coil. But using a LCR meter is not a practical method in our case. So we can measure the change in phase corresponding to the change in inductance. The most common and easy method to measure a phase is a Phase Sensitive Detector.

Phase Sensitive Detector

Basic principle of phase sensitive detector is an input sinusoidal signal fed into the PSD is multiplied by a reference sinusoidal signal of same frequency. The resultant signal is passed through a low pass filter. The output of the low pass filter is dependent on phase of the input signal. The circuit uses orthogonality of sinusoidal signal. Phase sensitive detector circuit can be implemented in many ways. Here we are using multiplier type PSD[11]. Let's look into the circuit of the phase sensitive detector(PSD)[12]. In 3.9 there are two signal sources V_X and V_R. V_X represent the input sinusoidal signal whose phase is to be measured and V_R represent reference signal which is also a sinusoidal signal. As mentioned earlier the circuit uses the orthogonality of sinusoidal signal. The same reference signal is fed into quadrature phase shifter. The frequency of the reference signal V_R should be same as that of V_X. If frequency of V_X is f_1 and frequency of V_R is f_2,where f_1 is not equal to f_2 then the output of the LPF will be zero. Also the integrating time of LPF must be two much longer than the period of the two signals. Mathematical representation of the circuit output is shown below

$$V_X = \sqrt{2}V_X sin(wt + \theta) \tag{3.45}$$

$$V_R = \sqrt{2}V_R sin(wt) \tag{3.46}$$

Output of the multiplier can be represented as follows
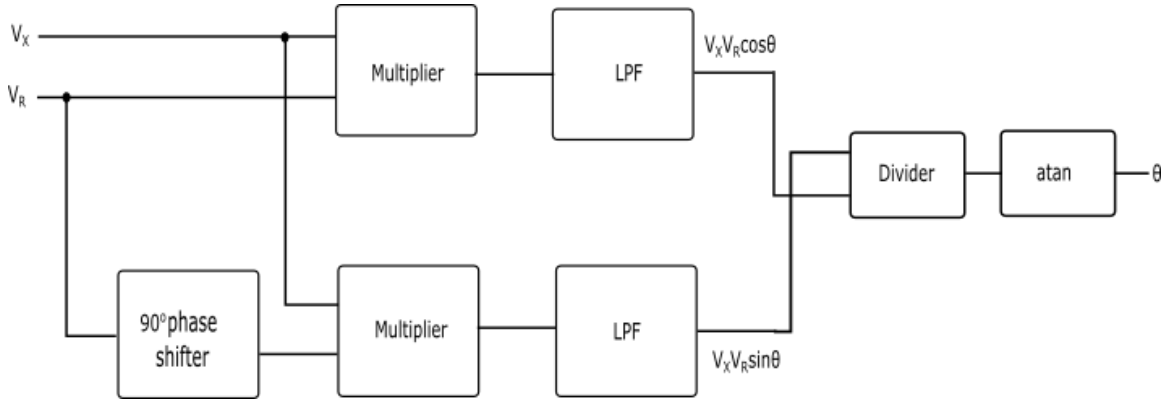
$$V_X.V_R = 2V_X V_R sin(wt + \theta)sinwt \tag{3.47}$$

Figure 3.9: Phase Sensitive Detector

Output of Low Pass Filter

$$V_P = \frac{V_R V_X}{T} \int_0^T [cos\theta - cos(2wt + \theta)].dt \tag{3.48}$$

$$= \frac{V_X.V_R}{T} cos\theta.T \tag{3.49}$$

$$= V_X.V_R cos\theta \tag{3.50}$$

Now let's consider the quadrature part.

$$V_q = \frac{2V_X V_R}{T} \int_0^T [sin(wt + \theta)sin(wt + 90].dt \tag{3.51}$$

$$= \frac{V_X.V_R}{T} \int_0^T [cos(\theta - 90) - cos(2wt + 90 + \theta).dt \tag{3.52}$$

$$= V_X.V_R sin\theta \tag{3.53}$$

Output of the circuit is represented below

$$\theta = tan^{-1}\left(\frac{V_q}{V_P}\right) \tag{3.54}$$

We used LabVIEW for implementing the multiplier type PSD which is shown in 3.10. let's elaborate main blocks in LabVIEW circuit diagram.

DAQ Assistant:DAQ assist is used to acquire data from an external source efficiently and quickly. We use NI Elvis as this external source on which the circuit is mounted. DAQ Assistant act as an interface between NI Elvis and LabVIEW programming environment.

Hilbert Transform:This block is used to make cosine signal from sine input signal.
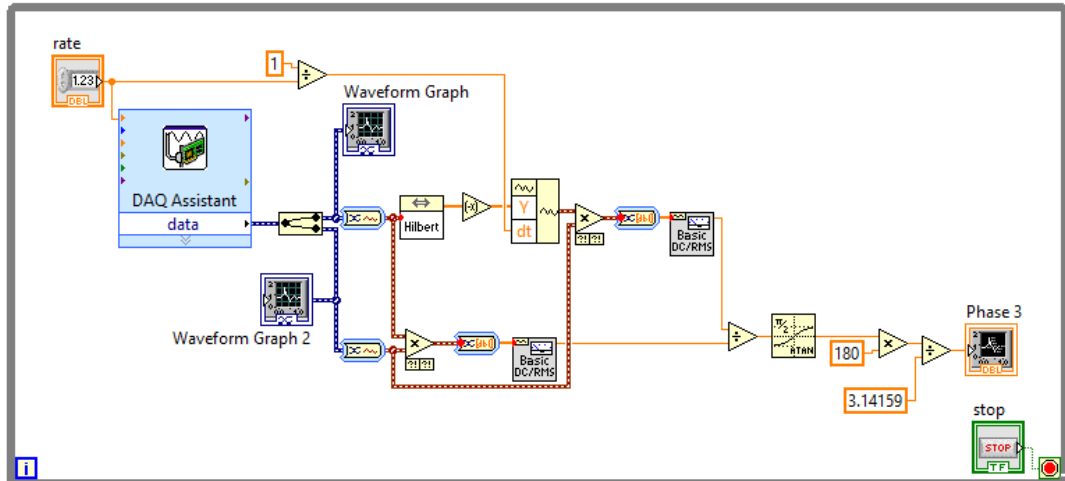
Figure 3.10: PSD in LabVIEW

As we all know Hilbert transform of sine gives negative cosine signal so an inverter is added after the Hilbert block.

Basic DC:This block is used instead of LPF because both will do similar action as far as our circuit is concerned.

Build waveform:While we compare block diagram given above and the labVIEW block diagram we can figure out this is an extra block. The reason for including this is basically the incompatibility of certain blocks with different data types of input. In our case the trouble maker is Hilbert block that works only for scalar input. So this scalar array should be converted back to the waveform. This block builds an analog waveform from the waveform components which are the scalar array.

Arctan:Output of the divider block is tangent of phase. This block is used to get the inverse tangent which is phase in radians. Further blocks that we can see in the diagram is for converting phase in radians to degree.

Linear Output

In the previous section we have seen that inductance changes as a cosine function of the displacement being sensed. Since the change in phase corresponding to the change in inductance is small we can do small angle approximation in and consider that phase change is directly proportional to change in inductance. Fig 3.11 shows the change in phase with respect to displacement. We are interested in an output that is linear. Former section of signal conditioning circuit shows the method of extraction of phase difference
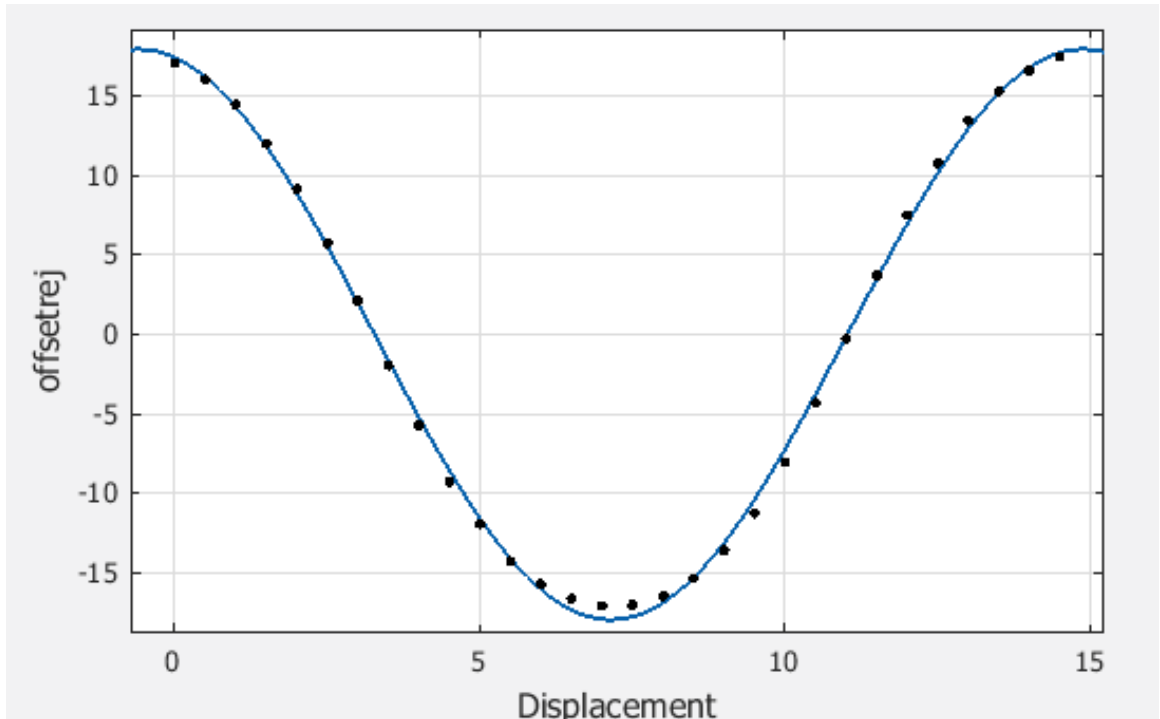
22

Figure 3.11: Phase change with respect to displacement of permalloy

Table 3.1: The table shows the mapping of linear displacement to radial displacement where L is the Diameter of the coil

Displacement(x in mm)	Angle(ϕ in radian)
0	0
L/4	$\pi/2$
L/2	π
3L/4	$3\pi/2$
L	2π

between input signal and output signal of RLC circuit. Now our objective is to extract inverse cosine from the PSD output. As seen in Fig3.11the x-axis is displacement. For simplifying the task we have to map displacement to angle. From the table3.1 we can find the mapping equation as

$$\phi = \frac{2d\pi}{L} \tag{3.55}$$

A basic block diagram of Linearization of cosine signal is given below in Fig3.12. The technique to obtain inverse cosine uses a reference signal which is also a sinusoidal signal $V_m sinwt$. Inputs to the comparator are reference sinusoidal signal in the positive terminal and $A\cos\phi$,where A is a constant and ϕ varies from 0 to π,in the negative terminal. We know V_c will be high whenever $V_m sinwt$ greater than $\cos\phi$ and will be

low otherwise. The comparator output V_c control the switch position. A dc reference voltage V_r is connected to terminal 1 of SPDT switch and ground voltage to the terminal 2. Output of the switch is given to the low pass filter.

Peak to peak amplitude of the reference signal is equal to the maximum phase change
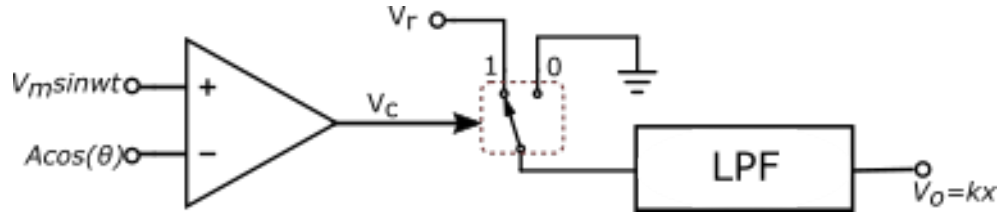

Figure 3.12: Functional block diagram that shows the phase linearization method

of the RLC network. Assume that the change in $kcosx$ is negligible over a period of time T,where $T = \frac{2\Pi}{\omega}$,ω is the angular frequency of reference signal. Consider a cycle(t=0 to t=T)of the reference signal. $Acos(\phi)$ will be positive in the range $0 \leq \phi \leq \frac{\pi}{2}(0 \leq x \leq \frac{L}{4})$.$V_c(t)$ will be zero from $t = 0$ to t=t_1,where $t_1 = \frac{1}{\omega}sin^{-1}\left(\frac{Acos(\phi)}{V_m}\right)$.Since $A = V_m$ the equation will become $t_1 = \frac{1}{\omega}sin^{-1}(cos\phi)$. As cosine function is positive in the specified range we can modify $cos(x) = sin(\frac{\pi}{2} - \phi)$. So

$$t_1 = \frac{1}{\omega}sin^{-1}\left[sin\left(\frac{\pi}{2} - \phi\right)\right] = \frac{1}{\omega}\left(\frac{\pi}{2} - \phi\right)$$

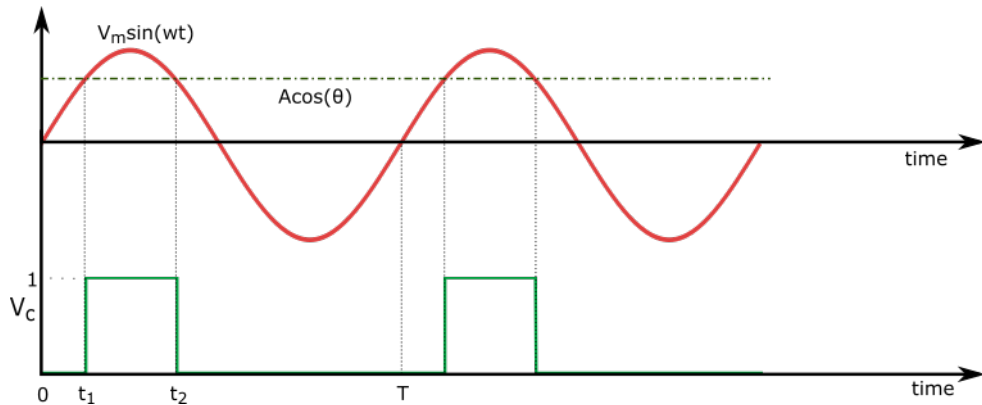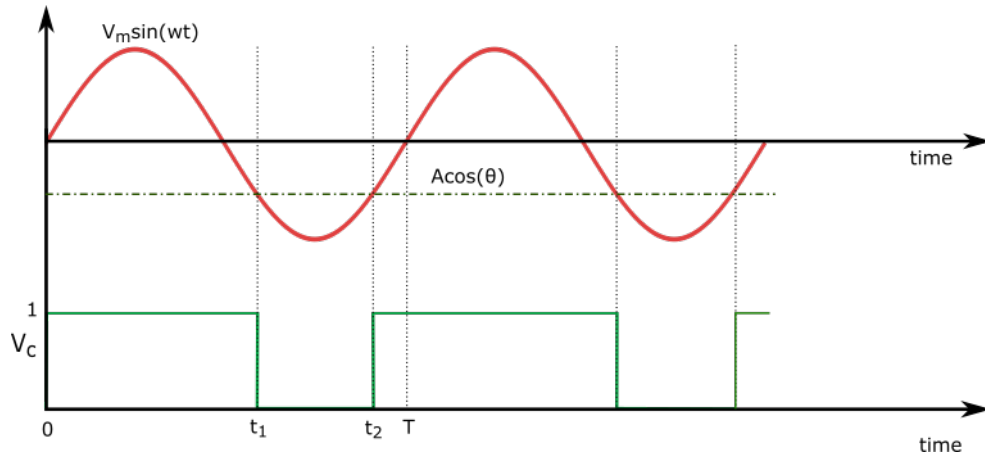
Figure 3.13: Diagram showing implementation of inverse cosine $V_m sin(\omega t)$ is the reference signal and $Acos(\theta)$ is positive in the range $0 \leq \theta \leq \pi/2$

In the Fig3.13. we can see that comparator output $V_c = 1$ in the range t_1 to t_2,where $t_2 = \frac{T}{2} - \frac{1}{\omega}sin^{-1}(cos\phi)$. This can be reduced to

$$t_2 = \frac{1}{\omega}\left(\frac{\pi}{2} + \phi\right)$$

24

The comparator output acts as a control signal signal for the SPDT. Switch selects V_r if V_c is 1 and selects ground terminal if V_c is 0. Now let us look at the output of LPF.

$$V_0 = \frac{1}{T}\left[\int_0^{t_1} 0\,dt + \int_{t_1}^{t_2} V_r\,dt + \int_{t_2}^{T} 0\,dt\right] \tag{3.56}$$

$$= \frac{V_r}{t}[t_2 - t_1] \tag{3.57}$$

$$= \frac{V_r\omega}{2\pi}[t_2 - t_1] \tag{3.58}$$

$$= \left(\frac{V_r}{\pi}\right)\phi \tag{3.59}$$

Substituting (3.49) in (3.53) we get,

$$V_o = \frac{V_R x}{\frac{L}{2}} \tag{3.60}$$

We can see that output voltage is directly proportional to the displacement(x). In

Figure 3.14: Diagram showing implementation of inverse cosine $V_m sin(\omega t)$ is the reference signal and $A cos(\theta)$ is negative in the range $\pi/2 \leq \theta \leq \pi$

Fig3.14 $Acos(\theta)$ will be negative in the range $\pi/2 \leq \theta \leq \pi$. V_c will be high from 0 to t_1 and t_2 to T but it will be zero from t_1 to t_2. Expression for t_1 can be derived as $t_1 = \frac{1}{\omega} sin^{-1}(cos(\phi))$. Substituting $cos(\theta) = sin(\pi/2 + \phi)$ we will get

$$t_1 = \frac{1}{\omega}sin-1\left(sin\left(\frac{\pi}{2} + \phi\right)\right) = \frac{1}{\omega}\left(\frac{\pi}{2} + \phi\right) \tag{3.61}$$

Similarly we can express

$$t_2 = (3T/2) - (1/\omega)sin^{-1}(cos\phi)$$

25

The above equation can be simplified as

$$t_2 = \frac{1}{\omega} \left(\frac{5\pi}{2} - \phi \right) \tag{3.62}$$

Now the output of LPF is

$$V_o = \frac{1}{T} \left[\int_0^{t_1} V_R dt + \int_{t_1}^{t_2} 0 dt + \int_{t_2}^{T} V_R dt \right] \tag{3.63}$$

$$= \frac{V_R}{T} [t_1 + T - t_2] \tag{3.64}$$

$$V_o = \frac{V_R}{\pi} \phi \tag{3.65}$$

By substituting (3.49) in the above equation

$$V_o = \frac{V_R x}{\frac{L}{2}} \tag{3.66}$$

So both (3.60) and (3.54) are same and are directly proportional to displacement x. Since V_R and L are static it does not influence the change in output.

The linearizing(inverse cosine) technique is practically implemented in LabVIEW as shown in Fig.3.15
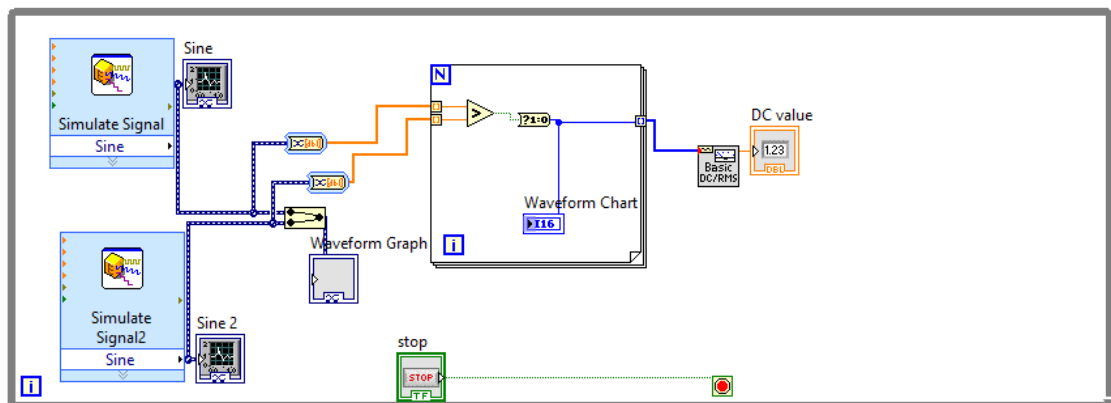
Figure 3.15: Inverse Cosine Technique using LabVIEW

Simulate Signal:This is reference sinusoidal signal with frequency 100Hz.

Simulate Signal2:This represent the sensor output that should be linearized. We know that the frequency of reference signal should be very much higher than that of sensor output. So we select a very low frequency of 0.0001Hz.

Comparator:The comparator is build using a while loop and a comparison block. Logic high of comparator is 1 and low is 0.

Basic DC:This will function as a LPF as we have seen in PSD.

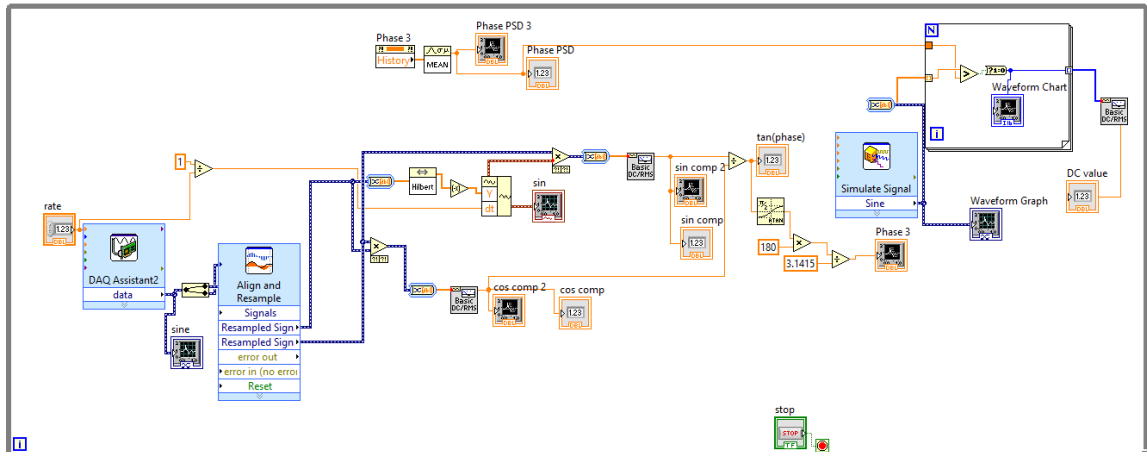Fig 3.16 shows the complete block diagram of labview VI. DC Value block gives the final output.

Figure 3.16: Block diagram of VI

3.3 Conclusion

Two signal conditioning circuits were designed and tested. Among the two, method-2 was simple and straight forward. It consist of a series RLC circuit, Phase sensitive detector and inverse-cosine linearization block. PSD and linearization blocks were realized using LabVIEW.

CHAPTER 4

EXPERIMENTAL RESULTS

Three coils were fabricated on PCB and tested. Excitation for RLC circuit was given by NI-ELVIS prototyping board. Data acquisition system in LabVIEW helped to acquire data from RLC circuit. Signal conditioning circuits were implemented in LabVIEW. Fig 4.1 shows the test setup. The obtained for different coils were documented here separately for easy comparison.
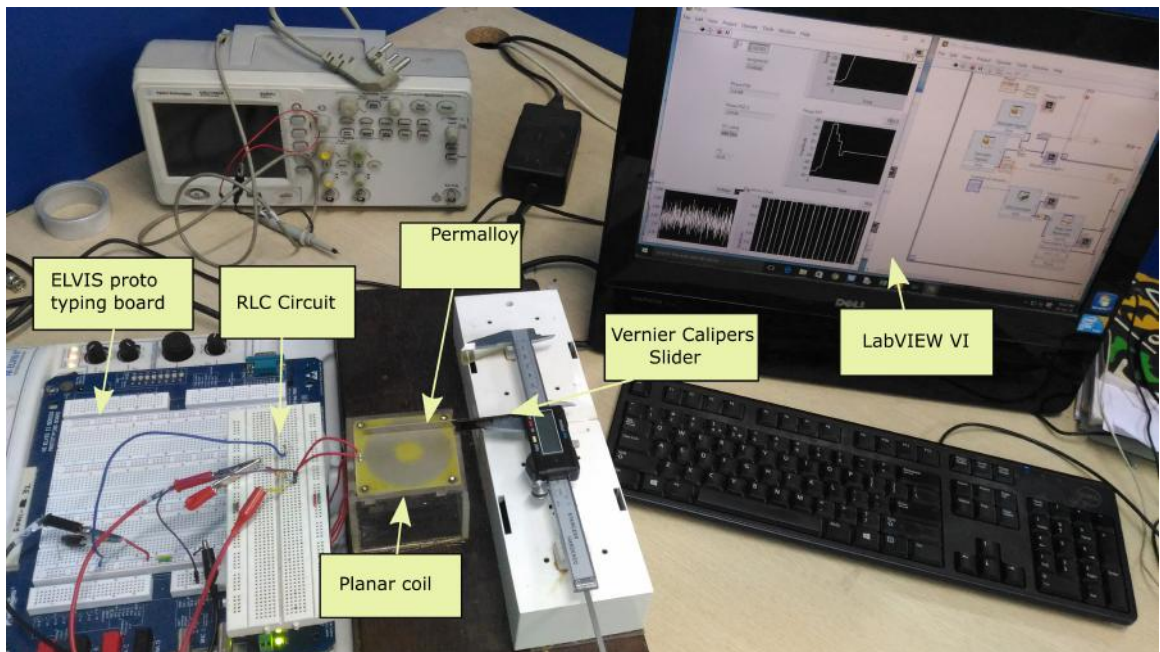
Figure 4.1: Test setup showing the ELVIS board,circuit,VI and coil-metal slider arrangement

4.1 Coil-1

Our first attempt was to find the inductance of the coil using LCR meter by placing the permalloy metal at different position of coil. Fig 4.2 shows the inductance value in the y-axis and displacement moved by metal in the x-axis.

Fig4.3 represent the sine fit of the change in phase. Carefully observing these figure we
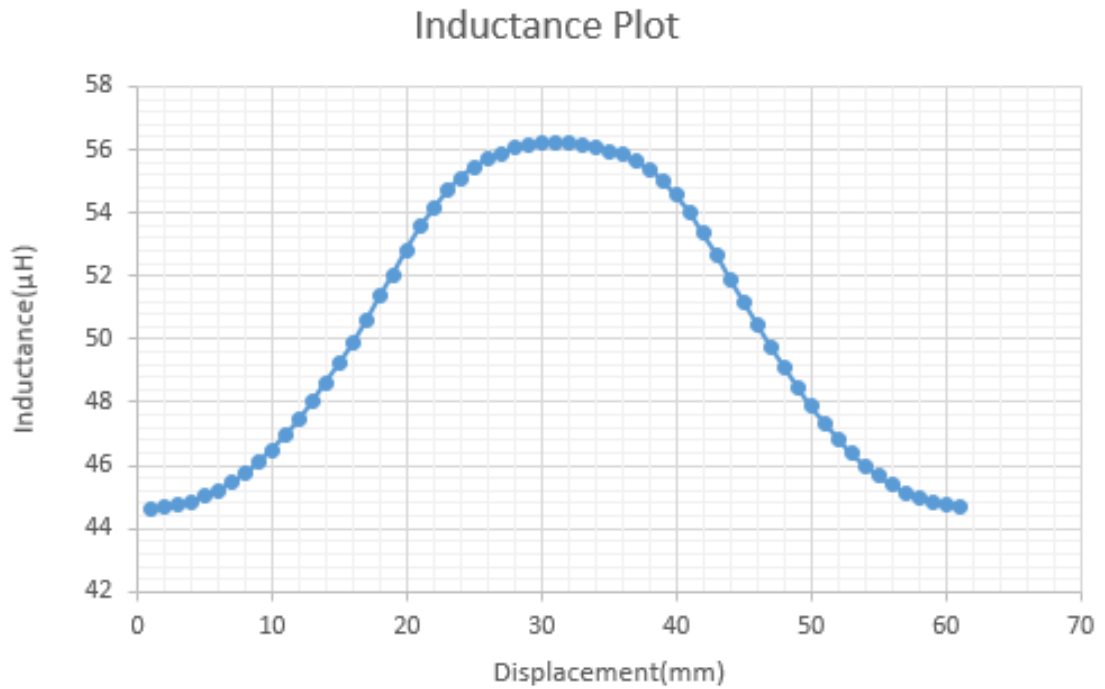
Figure 4.2: Inductance Plot of Coil-1

can figure out an unusual flatness at the top portion of the plot. It is the coil parameter
that is responsible for the dip. Since the inner diameter of the Coil-1 is large the induc-
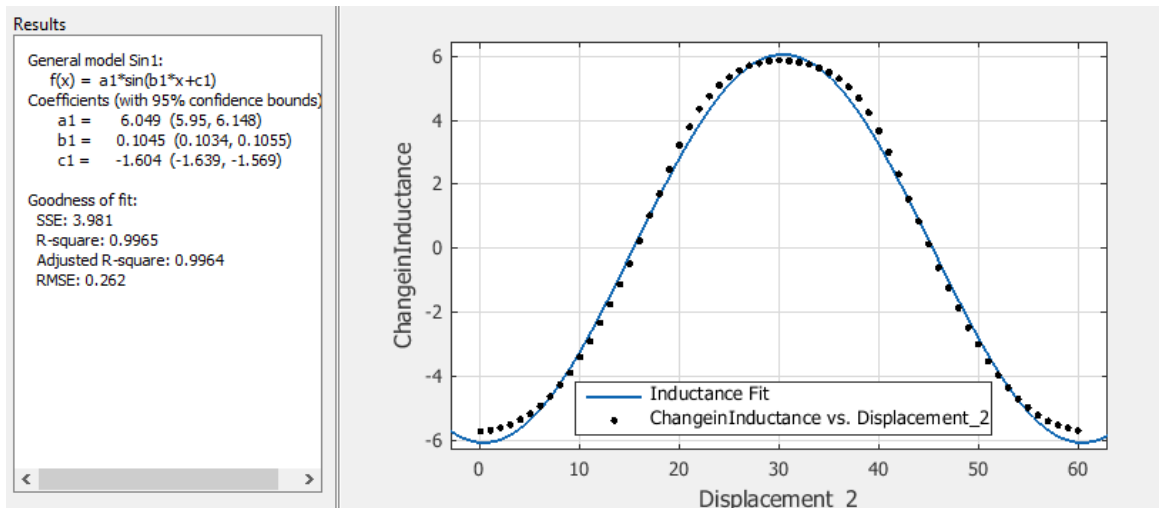tance values in the vicinity get reduced.

Figure 4.3: Sine fit of change in inductance

Fig. 4.4 and Fig. 4.5 shows the non-linearity in the output due to the dip in inductance
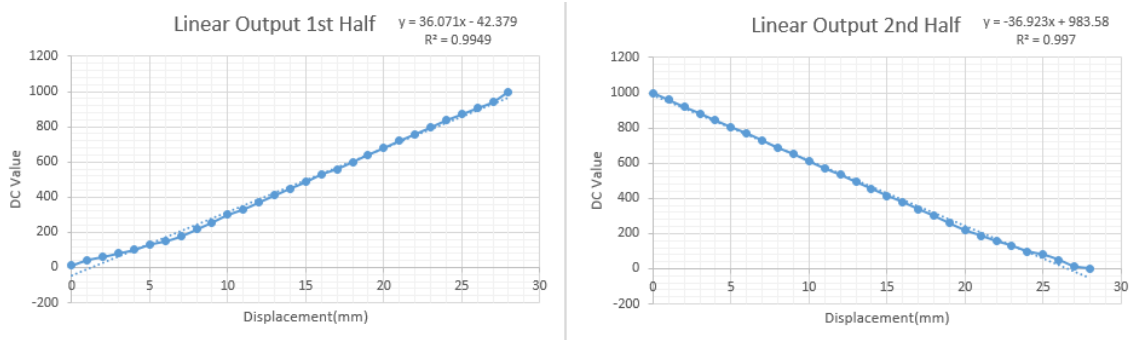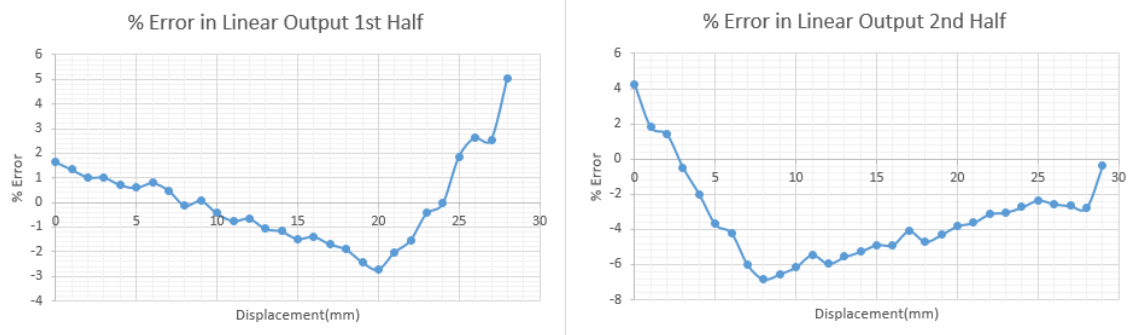value at the center of coil.

Figure 4.4: Linear Output of Coil-1

Figure 4.5: Percentage Full-Scale Error

4.2 Coil-2

Let's first analyze the change in inductance with displacement of the metal over the Coil-2. Fig 4.6 is the inductance plot of Coil-2.

The sine fit of Fig 4.6 is shown in the Fig 4.7.
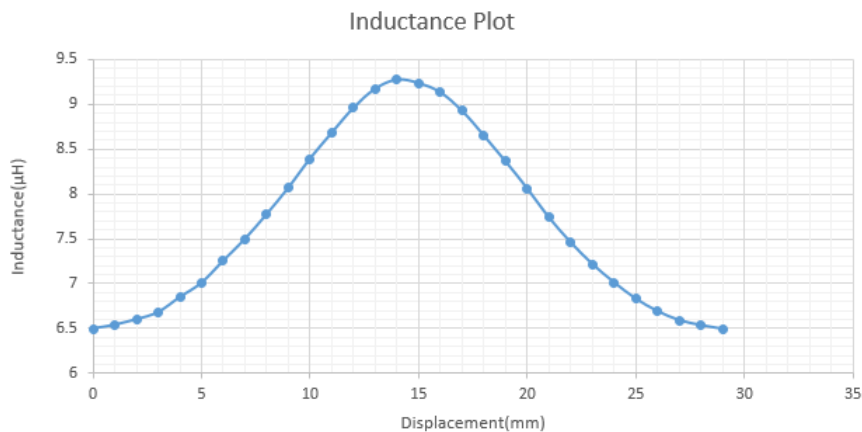
It is the offset rejected data that is plotted here.

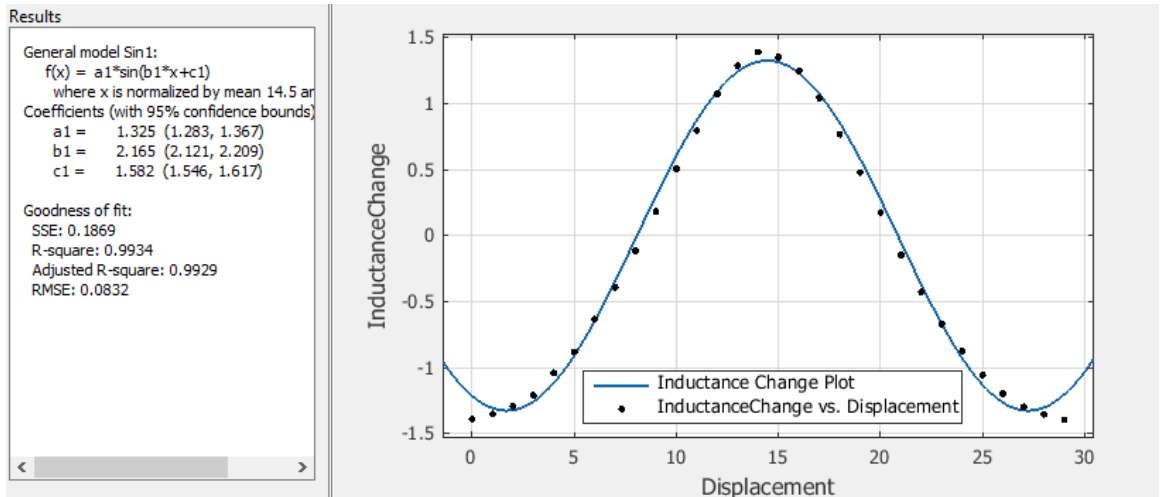Figure 4.6: Inductance Plot of Coil-2

30

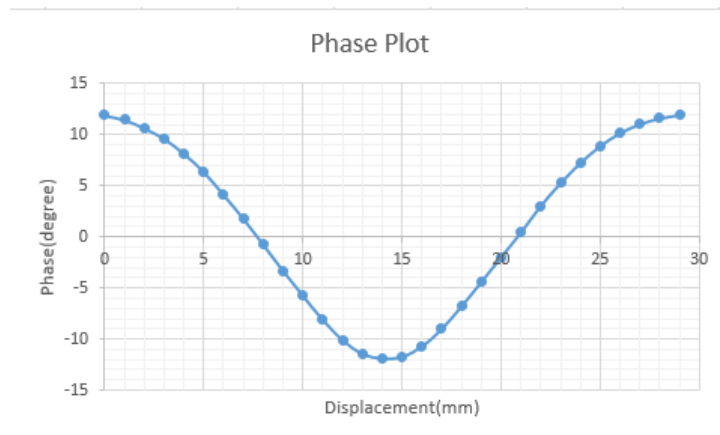Figure 4.7: Sine fit of change in inductance
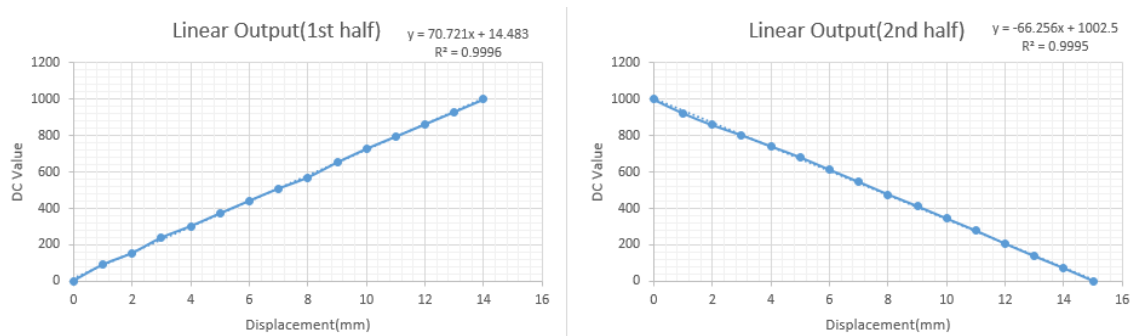

Figure 4.8: Phase plot

Figure 4.9: Linear Output

Following figures are the output of the signal conditioning circuit. We have mentioned earlier that phase should take a sinusoidal pattern as we could see in phase plot Fig4.8.

Now let's observe the final output that is the output of inverse cosine block Fig. 4.9. Linearized output is represented in two halves. From the linear fit of the Fig4.9 we
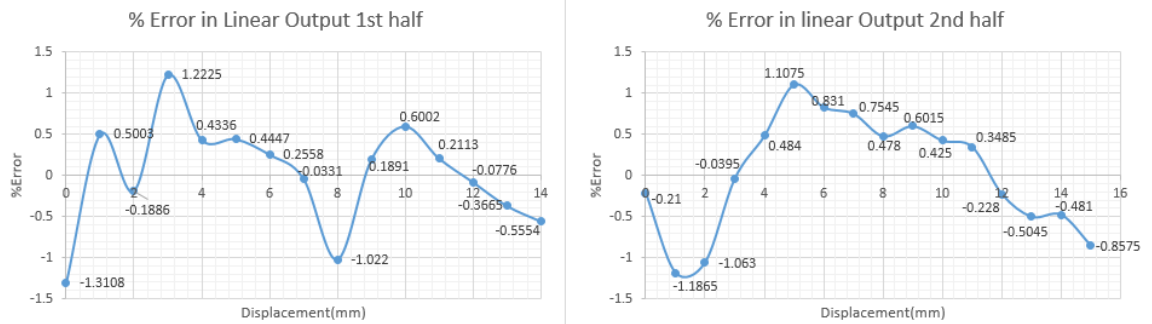
Figure 4.10: Percentage Full-Scale Error Plot

calculated the percentage error at every data points which is represented in Fig 4.10. Maximum error is 1.31% and there are 5 error points that are beyond 1%. Still the output is far better than that of Coil-1.

4.3 Coil-3

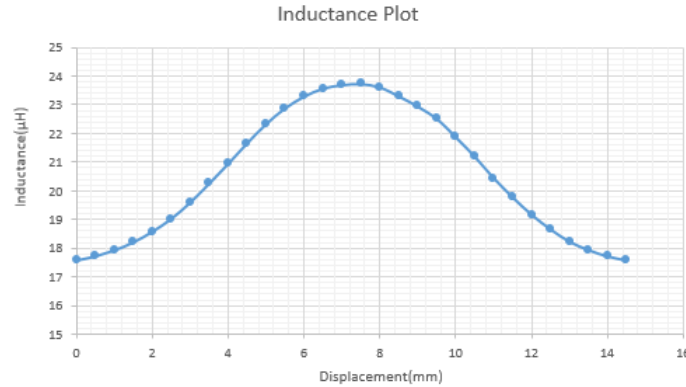The change in inductance with displacement is shown in Fig 4.11.

Figure 4.11: Inductance Plot of Coil-3

In Fig 4.12 we can see that the sine fit of change in phase with respect to displacement is pretty good. Phase plot is represented in Fig4.13. Phase that varies in sinusoidal pattern is linearized using the inverse-cosine block. The linear output is shown in Fig4.14. Percentage full scale error is given in Fig4.15. Maximum error is 1.89% and there are 10 error points that are beyond 10%.

So for every coil we are getting linear output with percentage full scale error greater than 1% which is not favorable since sensors having full scale error less than 1% are currently available in market. Now our attempt is to reduce the error.
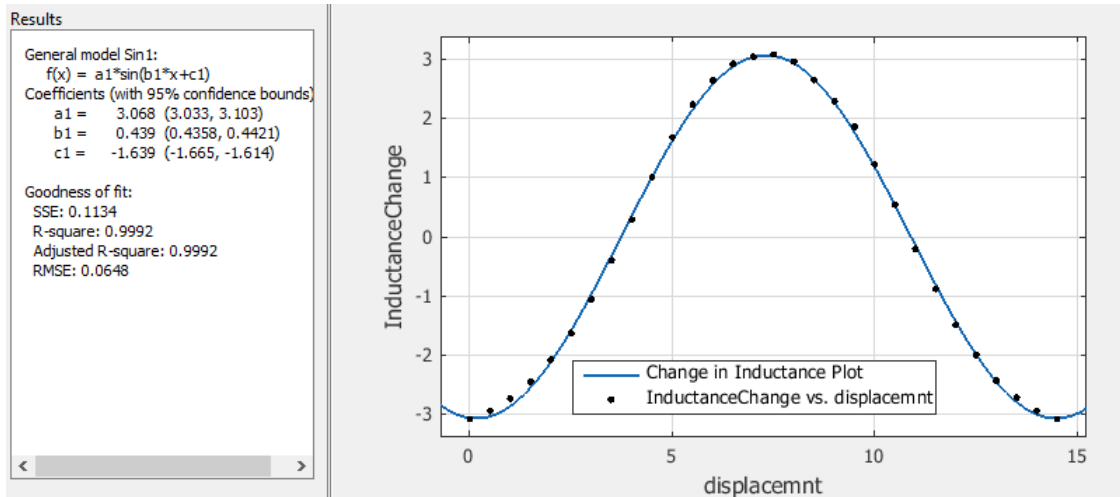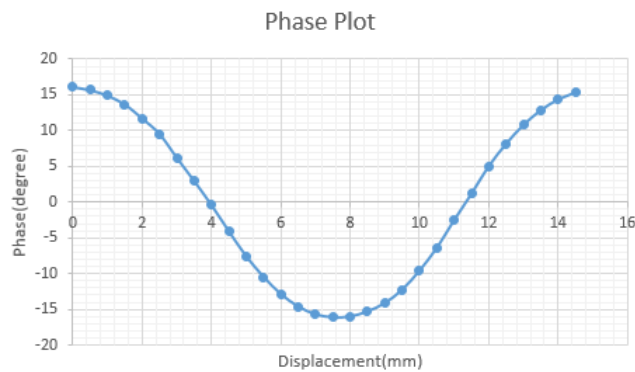
Figure 4.12: Sine fit of change in inductance

Figure 4.13: Phase Plot

Let's consider the Coil-3 to reduce its error. By close examination of the data we could find a peculiar pattern in plotting the error in phase change plot when compared to the sine fit of the same. The pattern was a third harmonic of the phase plot with lesser amplitude. The reason behind this pattern was the phase change pattern was a combination of a sinusoidal signal,that we considered earlier,and its third harmonics. Curve fit of phase plot is shown in Fig4.16.

Dots in Fig 4.16 are data points. Error between the phase plot data points and sine fit is calculated and plotted. Again a curve fitting is done for this error which is shown in Fig4.17. The curve fit gives a general model of the sinusoidal fit. Amplitude of the model is used to generate a 3rd harmonic sinusoidal signal. New reference signal is created using a sine signal generator block in LabVIEW. Fig 4.18 shows the comparison of new reference signal(New-Ref) and old reference signal(Ref). It is evident from the figure 4.18 that new reference signal resembles more with the phase plot.
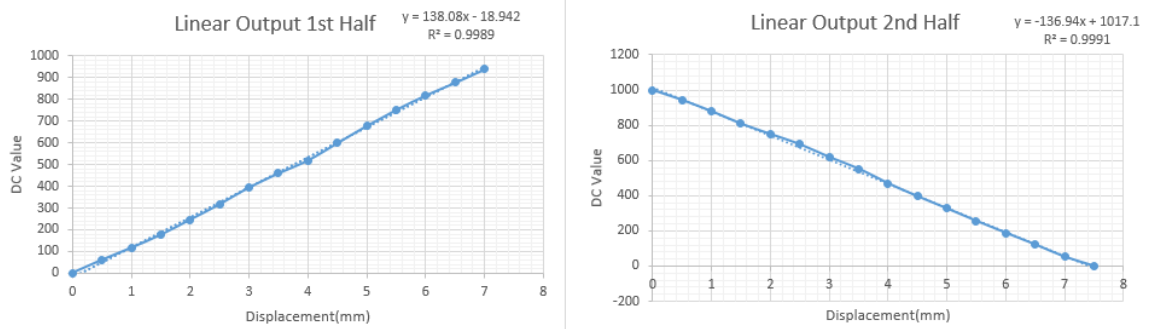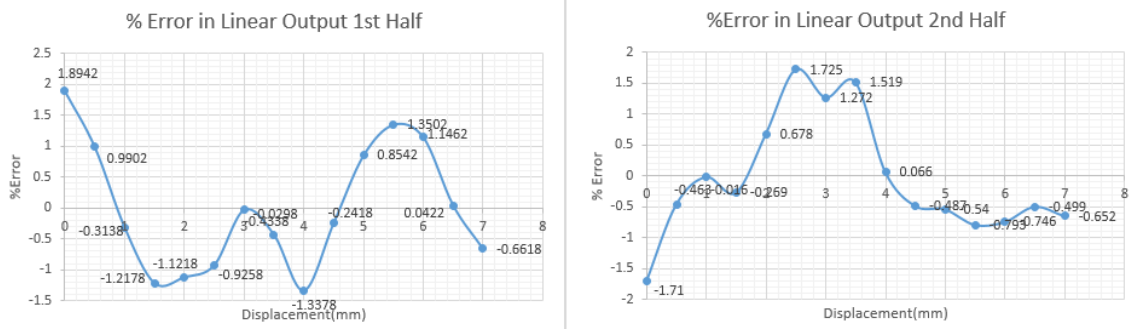
Figure 4.14: Linear Output

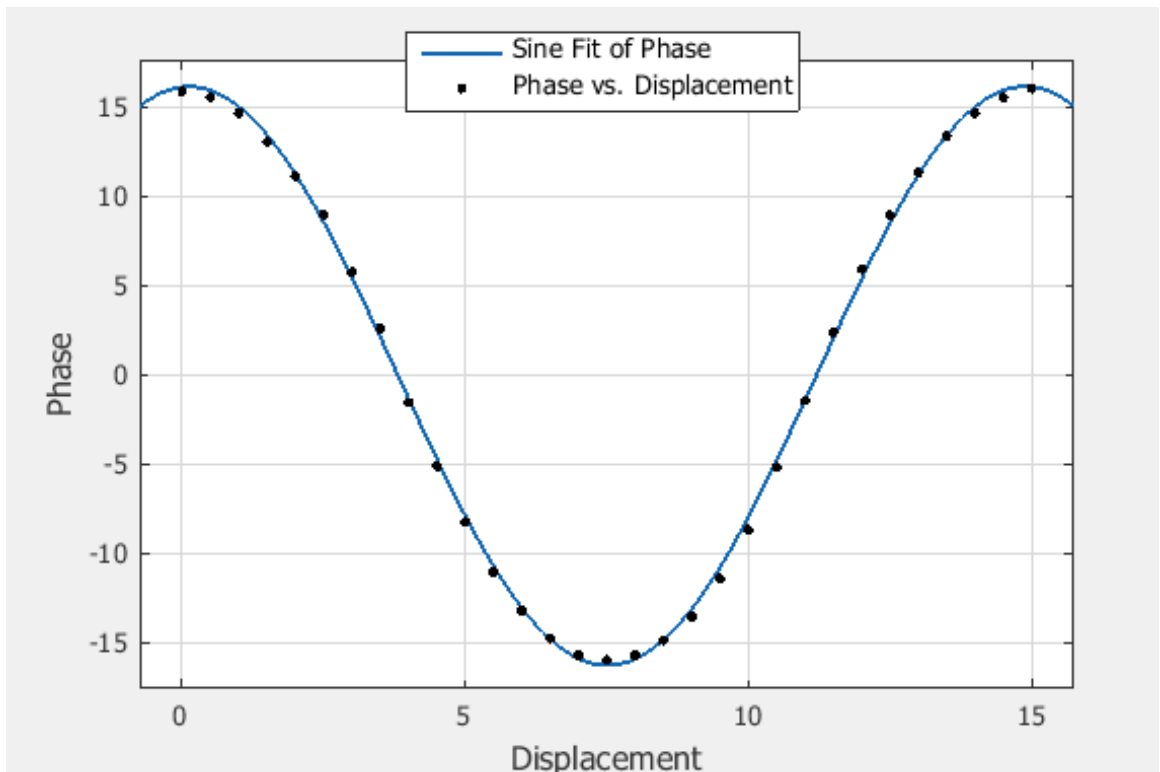

Figure 4.15: Percentage Full Scale Error

Figure 4.16: Sine fit of phase plot

The measurements are taken again with new reference signal. Fig 4.19 shows the improved linear output of the Coil-3.
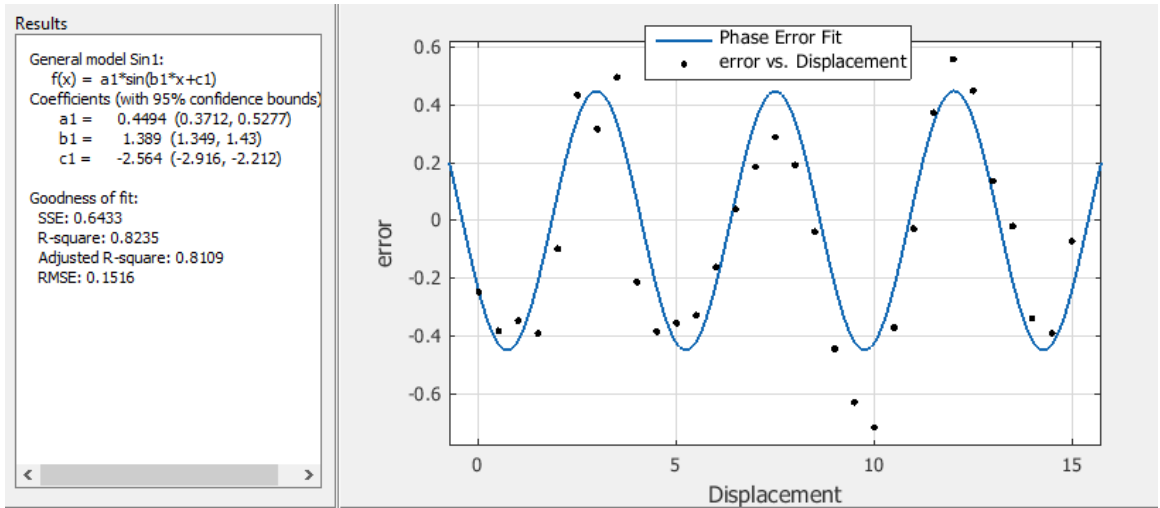
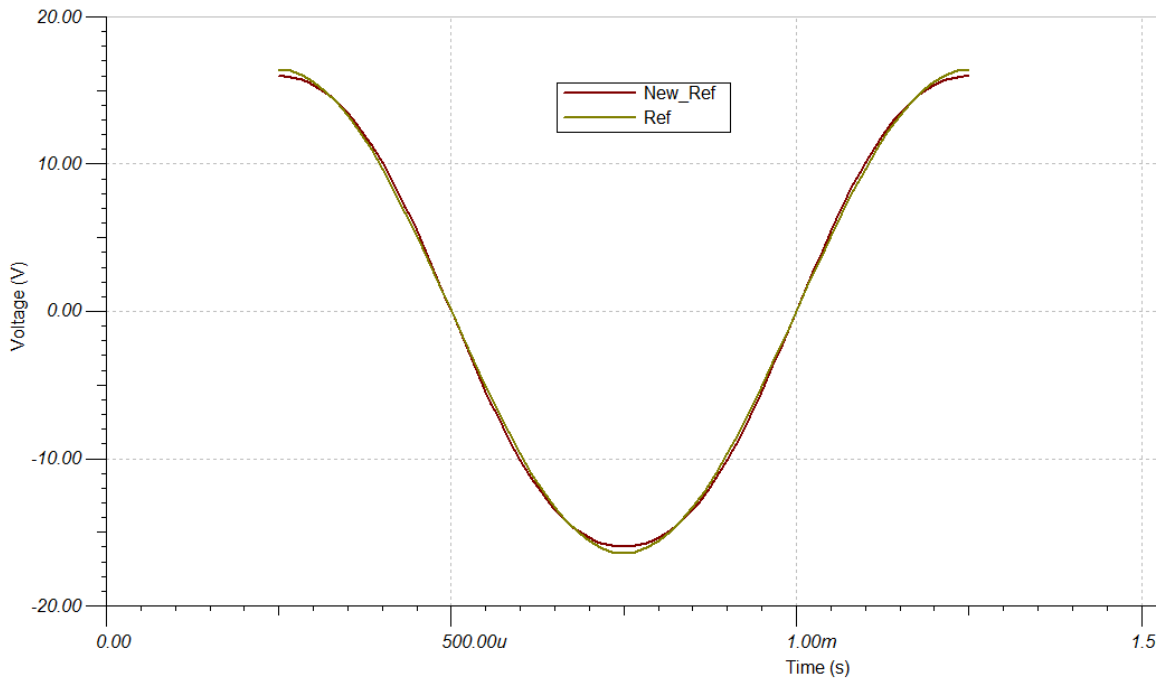Figure 4.17: Sine fit of Error in phase
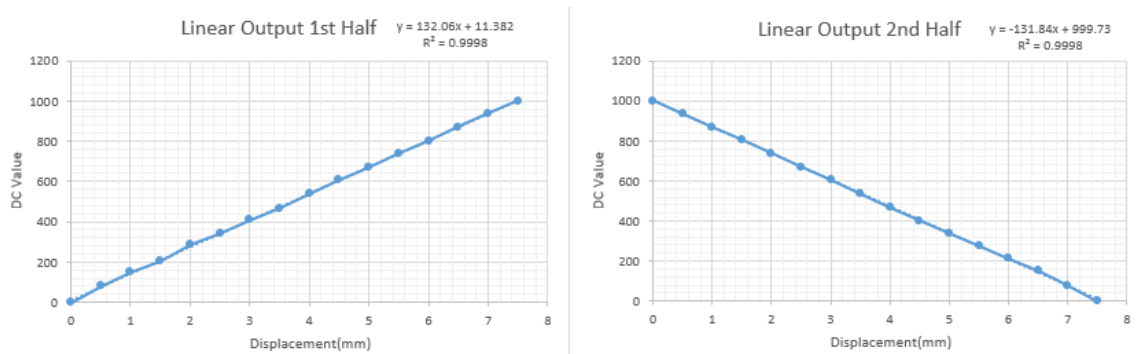

Figure 4.18: Comparison of reference signals

Figure 4.19: Improved linear output of Coil-3

Percentage full scale error of the improved linear output is shown in fig 4.20.We can find a large reduction in error except in the ends of the coil that is the initial and final data points. If we neglect this non-linear region we are getting a percentage full scale error less than 1%.
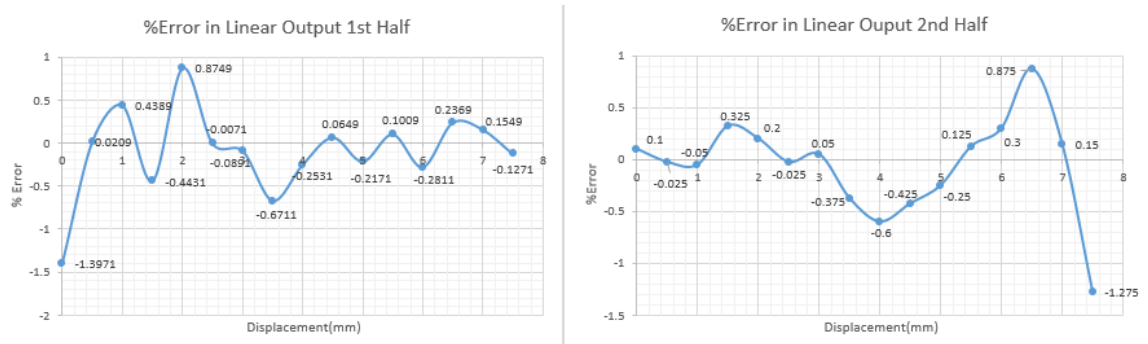

Figure 4.20: Sine fit of phase plot

This method can be implemented in other coils also to reduce the error. Once the amplitude of the harmonics of the reference signal is found we can simply add up to the reference signal.

4.4 CONCLUSION

Using signal conditioning circuits linear outputs of all the three coils were observed. Coil-2 and Coil-3 gave satisfactory outputs with error less than 1.5% whereas Coil-1 output was not good because of the design and fabrication problem of the coil. Next step was to reduce the full scale error less than 1%.Close examinations of the results lead to an observation that the phase change pattern is a combination of two signals, a sinusoidal signal and its third harmonics.So to get better linear output we modified the reference signal of linearization block by adding its third harmonics and obtained a full scale error less than 1%.

CHAPTER 5

CONCLUSION

5.1 SUMMARY OF THE WORK

An inductive displacement sensor with linear output was designed and developed. The sensor arrangement and circuitry are simple and robust. The first phase of work comprised of FEM simulation of sensor. Flux,Magnetic field distribution and desired parameter changes were observed. The results of simulation encouraged to develop the sensor prototype.

Second phase consist of development of signal conditioning circuits. Among the two signal conditioning circuits,the series RLC circuit was simple and straight forward. Phase sensitive detector and linearization system was also incorporated with RLC to complete the signal conditioning circuit. The last phase comprises of verification of results and error calculations. Unfortunately all three coils gave an output with non-linearity less than 2%. In order to reduce the non-linearity a thorough checking is done. We could find a problem of harmonics in phase change. This finding made us to think of improving the reference signal of inverse-cosine block. After improving the reference signal the error is improved to 1%.

5.2 Future Scope

The measuring range of the sensor is very much dependent on the physical size of the sensor head. To overcome this the system with a metal incline which is rigidly coupled to the target. The large displacement is mechanically converted into a small change of the displacement between the incline and active face of the sensor [1]. This method enables significant increase in measuring range.

The inductive displacement sensor can be used in various application in industrial,automation,medical etc. The sensor used for the determination of the acting point

of contact force in the foot of a humanoid robot can be replaced by the sensor we proposed [2][3].

We can reduce the error by adding the harmonics to the reference signal. Earlier section we have seen the reduction in error in mini-coil. This method can be used for any type of coil and the procedure is also the same.

REFERENCES

[1] Sorin Fericean and Reinhard Droxler,"New Non-contacting Inductive Analog Proximity and Inductive Linear Displacement Sensors for Industrial Automation"IEEE Sensors Journal, Vol. 7, NO. 11, November 2007.

[2] Snezana Djuric, Laszlo Nagy, Mirjana Damnjanovic,"Determination of the Acting Point of Contact Force in a Foot of Humanoid Robot Using Inductive Displacement Sensor".

[3] S. Duriu,L. Nad,B. Biberdziu,M. Damnjanoviu and Lj. Zivanov,"Planar Inductive Sensor for Small Displacement" PROC. 26th International Conference on Microelectronics (MIEL 2008), NIS, SERBIA , 11-14 May, 2008.

[4] Mirjana S. Damnjanovic, Ljiljana D. Zivanov, Laszlo F. Nagy, Snezana M. Djuric, and Branimir N. Biberdzic,"A Novel Approach to Extending the Linearity Range of Displacement Inductive Sensor",IEEE Transaction on magnetics,Vol. 44, No. 11, November 2008.

[5] Manfred Jagiella,Dr. Sorin Fericean,"Miniaturized Inductive Sensors for Industrial Applications",IEEE,2002.

[6] Manfred Jagiella,Dr. Sorin Fericean,Reinhard Droxler and Albert Dorneich,"New Magneto-inductive Sensing Principle and its Implementation in Sensors for Industrial Applications",IEEE,2004.

[7] M. Razi Mousavi1,R.Pakdaman Zangabad,S.Chamanian,M. Bahrami,"Simulation of novel Linear Inductive displacement Sensor",International Conference on System Engineering,2011.

[8] B. Romanowicz,Ph. Lerch,Ph. Renaud,E. Ful1in,Y. de Coulon,"Simulation of integrated electromagnetic device systems",Centre Suisse d'Electronique et de Microtechnique S.A.,Jaquet-Droz 1,2007 Neuchatel, Switzerland.

[9] http://www.espimetals.com/index.php/technical-data/175-permalloy-80

[10] Anoop Chandrika Sreekantan, Boby George, Varadarajan Jagadeesh Kumar,"Analysis of a tunnelling magneto-resistance-based angle transducer",IET Circuits Devices Syst., 2014, Vol. 8, Iss. 4, pp. 301-310.

[11] Pallas-Areny,Ramon and Webster,John G,"Sensor and Signal Conditioning",Wiley,2000

[12] C. S. Anoop and Boby George,"Electronic Scheme for Computing Inverse-Cosine and its Application to a GMR Based Angle Sensor",IEEE Transaction on Instrumentation and Measurement, Vol. 61, No. 7, July 2012.

CURRICULUM VITAE

Name   :   Vivek Gangadharan

Date of Birth   :   31 March 1991

Place of Birth :   Thalassery,Kerala

Education   :   B.Tech from Government Engineering College,Kozhikode

E-Mail   :   vivekgangadharan7@gmail.com